Available online at www.sciencedirect.com
SCIENCE DIRECT®
ELSEVIER
European Journal of Mechanics B/Fluids 21 (2002) 677–699
EUROPEAN JOURNAL OF MECHANICS B/FLUIDS

The evolution of an initially circular vortex near an escarpment. Part II: numerical results ☆

D.C. Dunn [1]

Department of Aeronautics, Imperial College, Prince Consort Road, London SW7 2AZ, United Kingdom

Received 20 December 2001; accepted 26 August 2002

Abstract

Dunn, McDonald and Johnson [6] have obtained leading-order analytical results for the motion of an initally circular, quasigeostrophic vortex, near an infinitely long escarpment using f-plane dynamics. In the limit that the vortex is weak (i.e., topographic vortex stretching dominates advection by the vortex), advection of fluid across the escarpment is inhibited and at short times the escarpment acts like a wall. On the other hand, if advection by the vortex dominates over topographic vortex stretching (i.e., an intense vortex), expressions for the trajectory of the vortex centre may be obtained. In this paper the contour advection scheme of Dritschel [2] is used to investigate the full range of vortex strengths.

It is found that the pseudoimage description of the motion of a weak vortex is accurate beyond the time for which linear theory is formally valid. The analytic prediction of the drift of intense vortices is also shown to be accurate. The physical mechanisms for the evolution of an intense vortex are identified. In particular there is a 'trapped region' near the vortex periphery, which protects the vortex from deformation, and a 'trailing eddy', which contributes to motion perpendicular to the escarpment. These features are similar to those found in recent analytical and numerical studies of vortex motion on the β-plane.

For the case of a moderate intensity vortex, advection by the vortex and topographic vortex stretching are equally important, and in this highly nonlinear case no theory is available. Contour advection simulations reveal that anticyclones located on the shallow side of the escarpment are able to cross the escarpment, while cyclones located on the shallow side are 'back-reflected' and move away from the escarpment. Moderate vortices undergo enhanced motion in the direction perpendicular to the escarpment, compared with the weak and intense vortices. These characteristics of the motion are associated with dipole formation, and are consistent with recent experimental and numerical studies of barotropic vortices near escarpment topography.

Keywords: Vortex dynamics; Topography; Geophysical fluid dynamics; Contour dynamics

1. Introduction

Dunn, McDonald and Johnson [6] (hereinafter referred to as Part I), have obtained analytic results for the motion of an initially circular, quasi-geostrophic (equivalent-barotropic) vortex patch near an escarpment using f-plane dynamics. Two time-scales arise naturally in the problem, namely the advective time scale, T_a, associated with swirl velocity of the vortex, and the wave time scale, T_w, associated with vortex stretching by the topographic gradient. Analytical progress is possible when the two time scales are well separated.

In a previous study Dunn, McDonald and Johnson [5], examined the motion of a singular vortex near an escarpment. In the limit $T_a \gg T_w$, the effect of the topography is dominant, i.e., the vortex is weak. The escarpment acts (at least for times large compared to the topographic wave time scale) like a wall, inhibiting cross-isobath motion, and the vortex drifts in the sense

☆ This work was supported by NERC under grant GT4/95/206/M.
E-mail address: d.c.dunn@bristol.ac.uk (D.C. Dunn).
[1] Present address: School of Mathematics, University of Bristol, University Walk, Bristol BS8 1TW, United Kingdom.

0997-7546/02/$ – see front matter
PII: S0997-7546(02)01209-8

of its image in the escarpment. This phenomenon was named the 'pseudoimage' of the vortex. For longer times it was found that when the vortex moves in the same direction as the topographic waves, non-decaying waves are radiated in the wake of the vortex. The vortex responds to this radiation by moving perpendicular to the escarpment. In Part I it was found that a weak vortex patch remains circular for short times, the topographic waves rapidly propagate away from the vortex and the motion is also in the sense if the pseudomimage. It was not possible to extend the analysis to times longer than the topographic wave time scale. Stern and Flierl [16] and Bell [1] find that weak barotropic (i.e., 'log') vortices near a potential vorticity interface due to piecewise constant shear flow, also fail to 'capture' the interface, instead moving parallel to it. It appears that the pseudoimage behaviour may be general for a weak vortex near a sharp potential vorticity interface.

In the limit $T_a \ll T_w$, i.e., an intense vortex, the swirl velocity of the vortex prevents the initial disturbance from dispersing as topographic waves. In Part I it was found that the intense vortex remains circular to leading order in the small parameter $S = T_a/T_w$. The swirl of the vortex moves fluid across the topographic gradient, generating secondary circulations, which in turn steer the vortex. Cyclones (respectively anticylones) initially drift away from the deep (shallow) region. The vortex rotates the secondary circulations, and at large times both cyclones and anticyclones move in the direction of the topographic waves. This behaviour is analagous to the motion of an intense β-plane vortex, where the seconday circulations are called 'β-gyres' (see, *inter alia*, Lam and Dritschel [14], Reznik [14], Reznik, Grimshaw and Benilov [15] and the numerous references therein). McDonald [11] obtained results for an intense singular vortex near an escarpment which differ from those in Part I only in the form of the angular velocity of the vortex, which appears explicitly in the solution. The drift velocity of an intense singular vortex in the direction parallel to the escarpment always matches a possible phase velocity of the topographic waves, and non-decaying waves are radiated as a result. The singular vortex responds to this radiation by a slow drift perpendicular to the escarpment. In Part I, it was not possible to investigate the long-term dynamics of an intense vortex patch analytically.

The present study was motivated by the limitations of modelling vortex motion near an escarpment by a singular vortex. A singular vortex is unable to change its shape as it evolves and this has implications for the ability of a singular vortex model to capture the features of more realistic vortex motion. The singular vortex always has an axially symmetric velocity field associated with it, so the effects of vortex deformation are absent. This implies that the description of the effects of vortex deformation on both the drift of the vortex, and on the advection of potential vorticity is incomplete. Moreover the possibility that the vortex decays in response to wave radiation is absent. In Part I analytical progress was only possible as long as the vortex remains circular, and even then only for the weak vortex and intense vortex limits. In the present paper, the full nonlinear equations are integrated using the contour advection scheme of Dritschel [2]. Results are obtained for the full range of vortex strengths.

First, the motion of a weak vortex is considered. The motion of a weak vortex patch near an escarpment will be compared to the motion of an equivalent patch near a wall in order to investigate whether the pseudoimage phenomenology describes the motion of the vortex. Second, the motion of an intense vortex is considered. The analytical predictions of Part I are tested, and the larger time behaviour is investigated. Third, the motion of moderate intensity vortices (i.e., $T_a \approx T_w$), for which there was no theory in Part I, is investigated. Dunn et al. [5] considered the motion of a moderate singular vortex near an escarpment using contour dynamics. The vortex tends to pair up with fluid that has crossed the escarpment and gained net relative vorticity, forming dipole-like structures. Compared to weak or intense singular vortices, these structures undergo enhanced motion perpendicular to the escarpment. Similar behaviour has been observed for barotropic vortices near an escarpment in recent laboratory experiments due to Zavala Sanson, van Heijst and Doorschoot [19]. It was shown that moderate intensity anticyclones located on the shallow side of the escarpment are able to 'climb' the topographic gradient, while cyclones located on the shallow side are 'back-reflected'.

For the purpose of brevity, the results many of the numerical simulations are not shown. The omitted plots are available in the more verbose thesis of Dunn [4].

2. Problem formulation and numerical method

Here the problem is recast in an alternative, but equivalent, form to that given in Part I. Quasigeostrophic dynamics for a single-layer fluid whose surface is free to deform (i.e., equivalent-barotropic) are assumed. The fluid layer containing the vortex has average depth D, reduced gravity g', and contains an infinitely long escarpment with constant height ΔD. Let f be the Coriolis parameter, and choose as the characteristic length scale, $L = R_D = (g'D)^{1/2}/f$, i.e., the Rossby radius. The non-dimensional, quasigeostrophic potential vorticity, which is a conserved quantity, is

$$q = \nabla^2\psi - \psi + Sh_B(y), \tag{1}$$

where ψ is the streamfunction, $h_B(y)$ is the nondimensional height of the topography, which is assumed to vary only in the y-direction and $S = \delta/Ro$. Here $\delta = \Delta D/D$ is the fractional height of the escarpment, and $Ro = U/fL$ is the Rossby number. The two numbers, δ and Ro are small parameters, but their ratio S may take the whole range of values. The streamfunction has

been nondimensionalised using the scale $Rof L^2$. The Rossby number, Ro, is a function of the distance of the vortex from the escarpment and should be calculated by using the velocity associated with the swirl of the vortex *at the escarpment*. This can be estimated from the structure of the vortex. In this paper, this can be done using the Bessel function structure of the vortex patch. The nondimensional time scale for the motion is the advective time scale $T_a = f^{-1}Ro^{-1} = L/U$ of the vortex, sometimes referred to as the eddy turnover time. The parameter S can be rewritten

$$S = \frac{L/U}{\delta^{-1}f^{-1}} = \frac{\delta}{Ro} = \frac{T_a}{T_w}, \tag{2}$$

which is the ratio of the advective time scale to the time scale, $T_w = (f\delta)^{-1}$, which is the topographic wave time scale Johnson [8], Johnson and Davey [9]). Hence S is a measure of the vortex intensity. The escarpment is aligned along $y = 0$,

$$h_B(y) = \frac{\mathrm{sgn}(y)}{2}. \tag{3}$$

By analogy with the β-plane, shallow fluid lies in the direction of increasing y. For convenience of description, the direction of increasing y is identified as north, and increasing x as east. In reality there is no preferential direction on the f-plane, so this choice is made simply so as to align the isobaths in the β-plane sense.The fluid motion is strictly *not* quasigeostrophic near $y = 0$, since there the topography has infinite gradient, so the flow must be three-dimensional near the escarpment. However, the present choice of topography is an attempt to model a sudden depth change, ΔD, i.e., the horizontal length scale of the depth change (say l) is such that $R_D \gg l \gg \Delta D$. This implies that the vertical velocity scales like $\Delta D/l \ll 1$. It is assumed that the three-dimensional effects near the escarpment are negligible and have no leading order effect on the dynamics.

The initial condition is a circular patch of uniform potential vorticity, which with the Rossby radius as the characteristic length scale, can be written,

$$\Omega_0 = \nabla^2\psi_0 - \psi_0 = -\alpha H(a - r), \tag{4}$$

where a is the patch radius, r is the radial distance from the vortex centre and $\alpha = \pm 1$ gives the sense of the circulation. For $\alpha > 0$ it is clockwise (anticyclonic) and for $\alpha < 0$ it is anticlockwise (cyclonic). The vortex is initially centred at $(0, L)$. The patch boundary, represented by the Heaviside function in (4), and the contour which initially lies along the escarpment, are both material lines which are advected with the flow, making this an ideal problem to be studied by the contour advection scheme of Dritschel [2]. In Part I analytical results were obtained in the limit $S \to \infty$ (a weak vortex), and in the limit $S \to 0$ (an intense vortex). When $S \approx 1$, the effect of the topography and advection are comparable, and the motion is highly nonlinear. The contour advection scheme enables the full range of values of S to be investigated.

Fig. 1(a) shows the initial condition. There are three contours in the problem. The first is the topographic contour T, which lies along $y = 0$. The second is the advected contour A, which initially coincides with T, but which deforms as the flow evolves. The third contour is the boundary V of the vortex patch. Initially,

$$q = \begin{cases} -S/2 & \text{for } y > 0, \text{ but outside } V, \\ S/2 & \text{for } y < 0, \text{ but outside } V, \\ -\alpha & \text{inside } V. \end{cases} \tag{5}$$

Eqs. (1) and (5) imply that subsequently

$$\nabla^2\psi - \psi = \begin{cases} -S & \text{in region (i)}, \\ S & \text{in region (ii)}, \\ -\alpha & \text{in region (iii)}, \\ 0 & \text{elsewhere}. \end{cases} \tag{6}$$

See Fig. 1(b) for a definition of the various flow regions. Note that region (iii) is only properly defined so long as no part of the vortex crosses the escarpment. In such cases the potential vorticity gain by the vortex has to be taken account of. The velocity field is determined by inversion of (6) using Green's theorem, which gives for the point (x, y)

$$(u, v) = \frac{S}{2\pi}\int_T K_0(r)\,\mathrm{d}\mathbf{x}_k - \frac{S}{2\pi}\int_A K_0(r)\,\mathrm{d}\mathbf{x}_k - \frac{\alpha}{2\pi}\int_V K_0(r)\,\mathrm{d}\mathbf{x}_k, \tag{7}$$

where r is the distance from (x, y) to the point (x_k, y_k) on the contour being integrated over. The kernel, $K_0(r)$, is the modified Bessel function of the first kind, zeroth order. The contour nodes are advected by a fourth-order Runge–Kutta scheme, and the nodes are redistributed at each time-step using a nonlocal node-density function. Surgery is performed at a prescribed scale. See Dritschel [2] for full details of the algorithm. The unit of time in the simulations is T_a, the time scale associated with the swirl of the vortex; in the following discussion, T_a is often referred to as the eddy turnover time.

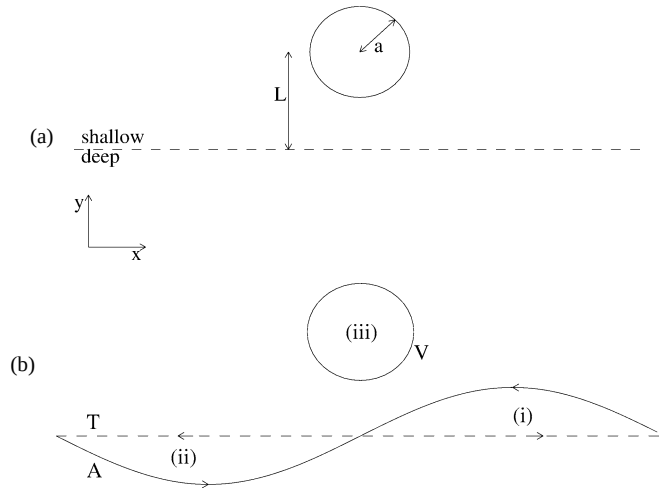

Fig. 1. The various regions of the flow. (a) Initially the topographic contour, T and the advected contour A coincide along $y = 0$. The variable potential vorticity $\nabla^2\psi - \psi$, is zero everywhere, fluid of high ambient potential vorticity lies in $y > 0$ and that of low ambient potential vorticity is in $y < 0$. Any initial deflection of the advected contour is solely due to the vortex, which is 'switched on' at time $t = 0$. (b) At subsequent times the fluid may lie in four types of region. In (i), above the topographic contour, but below the advected contour, fluid has moved from deep to shallow water and has $\nabla^2\psi - \psi = -S$. Fluid in regions such as (ii), below T but above A, similarly have $\nabla^2\psi - \psi = S$. Inside the vortex patch (iii), $\nabla^2\psi - \psi = -\alpha$, so long as no part of the vortex crosses the escarpment, in which case that part of the vortex has $\nabla^2\psi - \psi = -\alpha + S$. Elsewhere $\nabla^2\psi - \psi$ remains zero.

An inherent problem when computing the evolution of an infinite length contour is the need to use a finite length contour in practice. The topographic waves reach the end of the contour in finite time, a problem which is exacerbated when the vortex is weak. One solution is to damp the ends of the contours; this has been done in the present case by multiplying the y coordinate of the contour by a tanh function which falls to zero at the end of the contour. This implies that energy is removed from the computational domain. The damping is carried out many vortex radii from the vortex, and the oscillations which are damped are very small by the time they reach the damping region. However, energy conservation is not a good check on the integrity of the calculations. Physically, energy is eventually propagated infinitely far from the vortex, and the damping might be supposed to mimic this process. Conservation of the area of the vortex has been tested with the surgery algorithm switched off, and in all cases the area was conserved to machine accuracy. Other checks on the code include use of a vortex of zero strength, an escarpment of zero height, and an initially disturbed topographic contour in the absence of a vortex. These checks produce the expected results. Moreover, essentially the same code was used by Mc Donald and Dunn [12] to study a vortex near a seamount, and in that case the code does conserve energy.

Attention is restricted to the case $L > 0$, i.e., to vortices (of both signs) located on the shallow side of the escarpment. This represents no loss of generality, since the motion is invariant under the transformation

$$\psi(x, y) \to -\psi(x, -y). \tag{8}$$

Analogous results for vortices located on the deep side of the escarpment may be deduced by symmetry. The behaviour of anticyclones differs from that of cyclones, so the cases are treated separately. The trajectory of the vortex is taken to be that of the centroid $(x_c(t), y_c(t))$ of V:

$$x_c = \frac{\iint_V x\,\mathrm{d}x\,\mathrm{d}y}{\iint_V \mathrm{d}x\,\mathrm{d}y}, \qquad y_c = \frac{\iint_V y\,\mathrm{d}x\,\mathrm{d}y}{\iint_V \mathrm{d}x\,\mathrm{d}y}, \tag{9}$$

which initially coincides with the centre of the vortex patch. If V is broken up by surgery, then, following Lam and Dritschel [10], the contour enclosing the largest area containing fluid from the original vortex is used in this definition. Jumps, when they occur, can be smoothed out by altering the threshold at which surgery is carried out (costing more nodes in the calculation), or by reducing the time step (costing more in cpu time). In the present case the time step has been adjusted until no there is discernable difference in the trajectory of the vortex centroid. The vortex trajectories presented below do not exhibit any jumps.

3. A weak vortex patch

For convenience, in this section the parameter $\varepsilon = S^{-1}$ is used. In Part I, under the assumption that ε is a small parameter (i.e., a weak vortex), linear theory predicted that that the vortex patch would remain circular to leading order in ε, and drift in the sense of its pseudoimage for times $t \approx \varepsilon$. For large times, even linear theory is inhibited by the need to account for shape changes to the vortex. Indeed, a general theory of the evolution of a vortex near a wall is difficult for the same reason. Because of the impermeability condition at the wall (or equivalently, because of the influence of the image vortex), the streamlines cannot remain circular, and so the vortex shape must change. There is a family of vortices which maintain their shape, the so-called *V-states* of Pierrehumbert [13].

If there is no precise theory of a pseudoimage in this case, then a reasonable question to ask instead is "does the *phenomenology* of the pseudoimage explain the evolution of a weak vortex patch near an escarpment?". It is straightforward to calculate the evolution of a vortex near a wall, also by contour dynamics, and to compare this with the evolution of a vortex

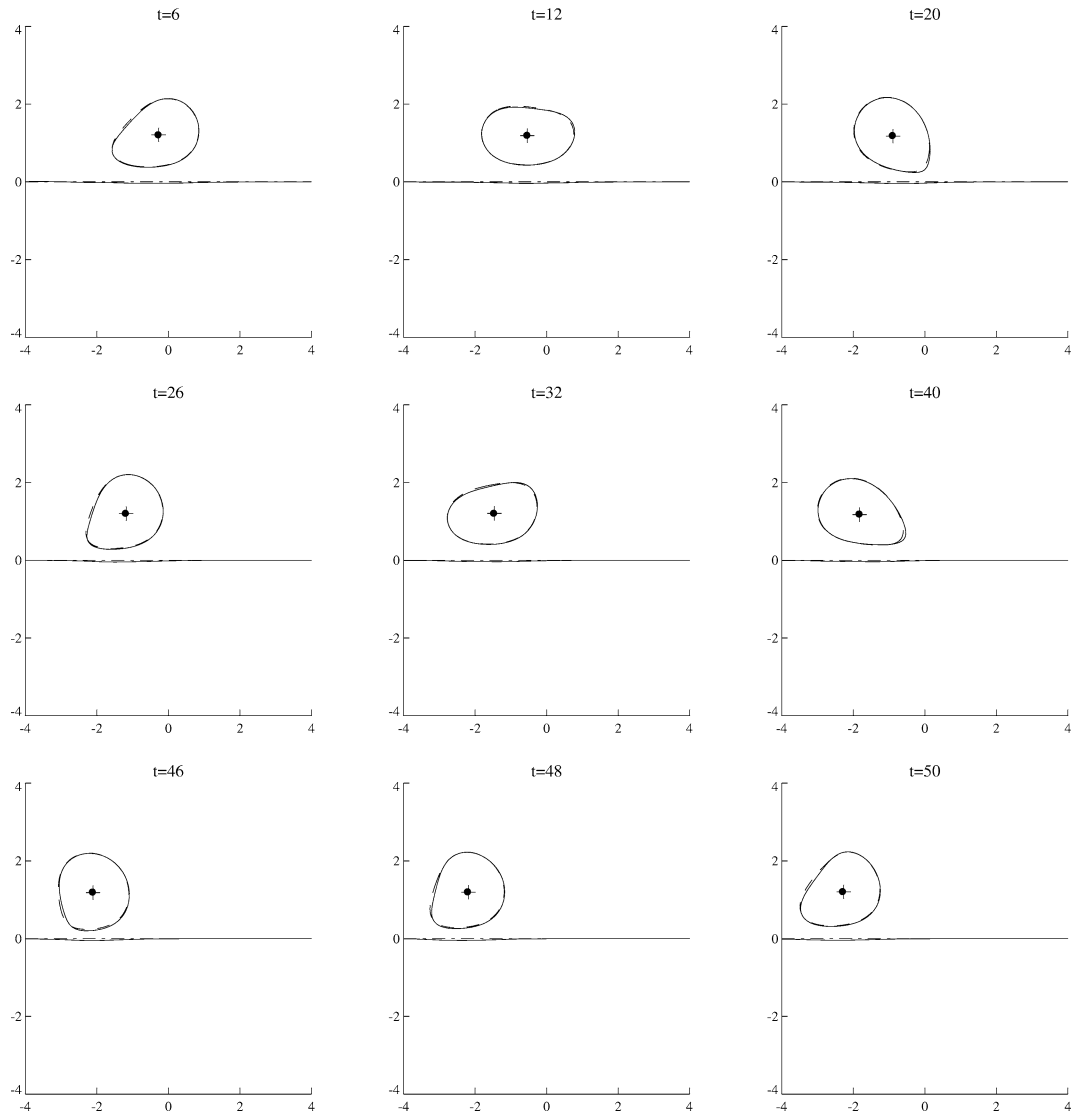

Fig. 2. Comparison of the evolution of a vortex patch near an escarpment (solid line) with that of a vortex patch near a wall (dashed line). The centroid locations are shown by a cross (escarpment) and a dot (wall), and the parameter values used are $\alpha = 1$ (anticyclone), $a = 1$, $L = 1.2$ and $\varepsilon = 0.1$. The topographic contour, T, is shown by a dot-dashed line. The advected contour, A, which initially lay over the escarpment is also shown with a solid line. The contours T and A almost coincide on the scale of this plot, but see Fig. 5.

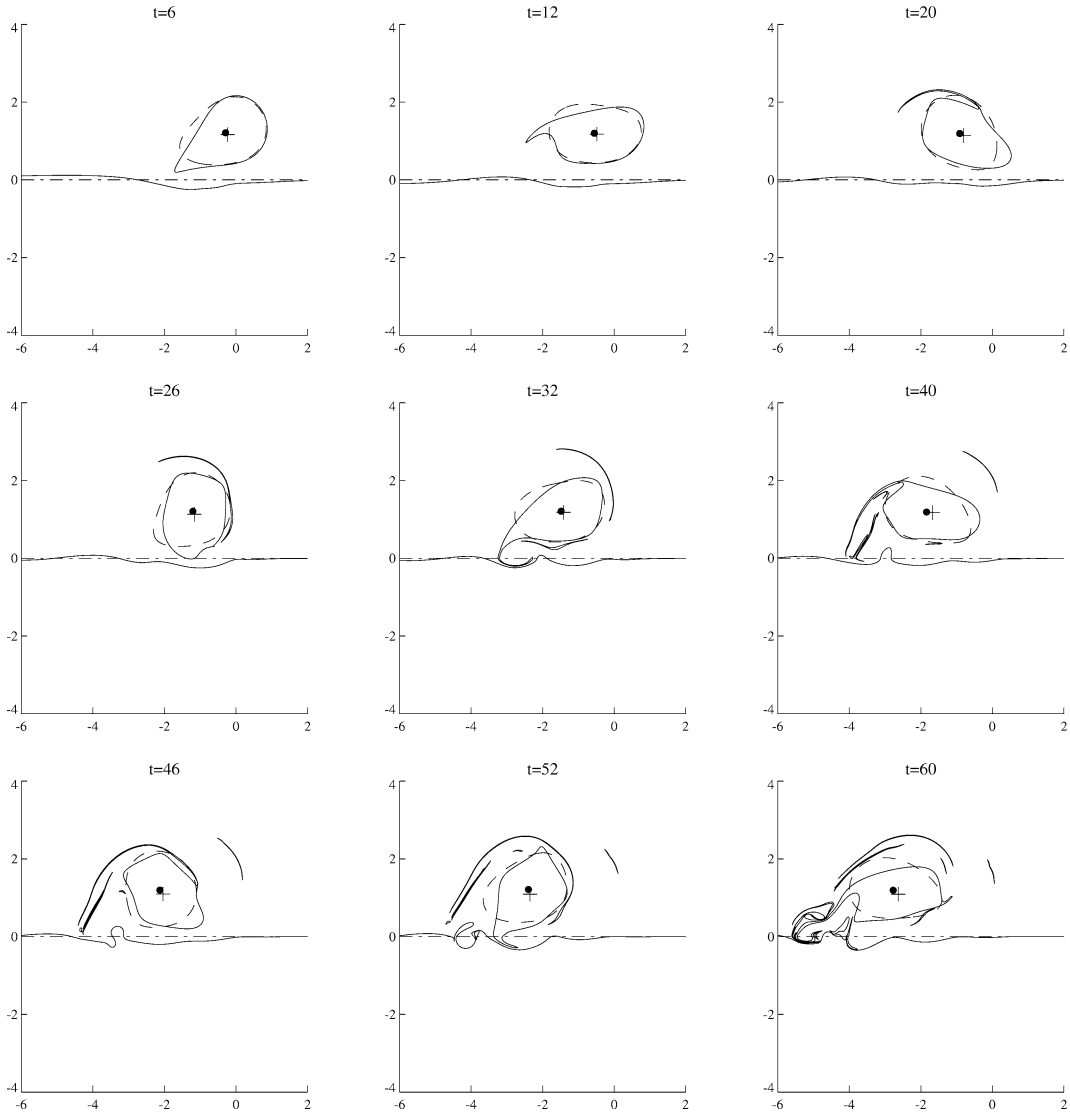

Fig. 3. As Fig. 2 except $\varepsilon = 0.4$.

near an escarpment. There are then two specific questions. First, does the pseudoimage predict the drift of the vortex centroid? Second, does the pseudoimage predict the shape of the vortex for $t > 0$. These questions are answered in the rest of this section.

3.1. Weak anticyclones

Fig. 2 shows a comparison between the evolution of an anticyclonic vortex patch near an escarpment with that of an equivalent anticyclonic vortex patch near a wall, for $\varepsilon = 0.1$. In each case $\alpha = 1$, $a = 1$ and $L = 1.2$. The patch near the escarpment is shown by the solid line, and its centroid by a cross. The patch near a wall is shown by the dashed line and its centroid by a dot. It is clear that the weak vortex patch evolves almost precisely in the sense of its pseudoimage for small ε. Both the patch boundary and the centroid are practically coincident with those of the patch evolving near a wall. This feature is robust, the calculation proceeding to 50 eddy turnover times, (i.e., well beyond the time for which linear theory is formally valid), without any significant deviation.

For $\varepsilon = 0.2$ (not shown), there are some small deviations in the vortex boundary compared with the pseudoimage prediction, and the beginning of some filamentation, usually associated with the presence of shear. This process is more clear in Fig. 3, which shows the contour evolution for $\varepsilon = 0.4$. The centroid location is less well predicted by the pseudoimage. The

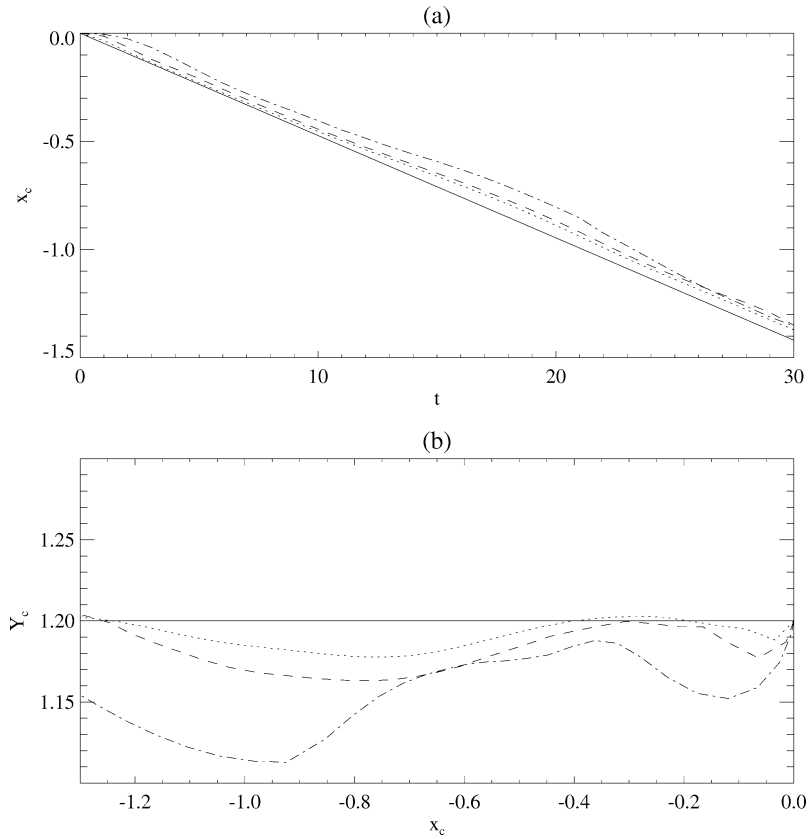

Fig. 4. Comparison of the drift of the weak anticyclones with the analytical prediction. The analytical prediction is shown by the solid line. The parameter values used are $a = 1,\ L = 1.2$ and $\varepsilon = 0.1$ (dotted line), $\varepsilon = 0.2$ (dashed line) and $\varepsilon = 0.4$ (dot-dashed line). The x_c-coordinate is shown in (a) as a function of time, and the centroid trajectories in (b).

filamentation of the patch boundary, and its deformation from the shape predicted by the pseudoimage theory is clear. At later times the vortex patch is ripped apart, and fluid initially located within the vortex boundary is entrained by the topographic waves and disperses away from the vortex.

Fig. 4 shows the drift of the vortex centre for $\varepsilon = 0.1,\ 0.2$ and 0.4. Also shown is the predicted drift,

$$u = \varepsilon\alpha a I_1(a) K_1\big(2|L|\big)\operatorname{sgn} L, \qquad v = 0, \tag{10}$$

derived in Part I (Eqs. (56) and (57)), under the assumption that the vortex remains circular. As expected the agreement with the theory improves with smaller ε. Dunn et al. [5] obtained a similar solution for the motion of a weak singular vortex for very short times, but were then able to show that the pseudoimage also dominates the motion on the longer, advective time scale. Consider their Figs. 7 and 10, which show almost purely zonal drift of weak vortices after the initial spin-up of the pseudoimage. In the present case, restricting attention to $\varepsilon = 0.1$, the anticyclonic vortex patch centroid undergoes much more of an oscillating drift than a singular vortex of the same strength. It would be easy to conclude that this drift is due to the influence of the topographic waves. However, for formally the same solution as in Eqs. (53), (54) in Part I, Dunn et al. [5] showed that the topographic waves have no influence on the vortex trajectory for times of order 1 on the advective time scale (see their Eq. (3.21)). Moreover, the vortex centroid near a wall (Fig. 2) undergoes the *same* oscillatory drift as the vortex near an escarpment. Hence, for small ε, it may be concluded that the response remains linear for $t = \mathrm{O}(1)$, and that the deviation from the purely zonal drift predicted in Part I is due to the vortex not remaining circular, rather than the nonlinear interaction of the vortex with the waves. For larger ε the waves are likely to be partially responsible for the enhanced oscillations: the same type of oscillations are seen for less weak singular vortices in Dunn et al. [5].

To understand how linear theory fails, it is useful to consider the evolution of the topographic contour, which is shown in Figs. 5 and 6 for $\varepsilon = 0.1$ and 0.4, respectively. Johnson and Davey [9] showed that the topographic waves in this domain have phase and group velocities

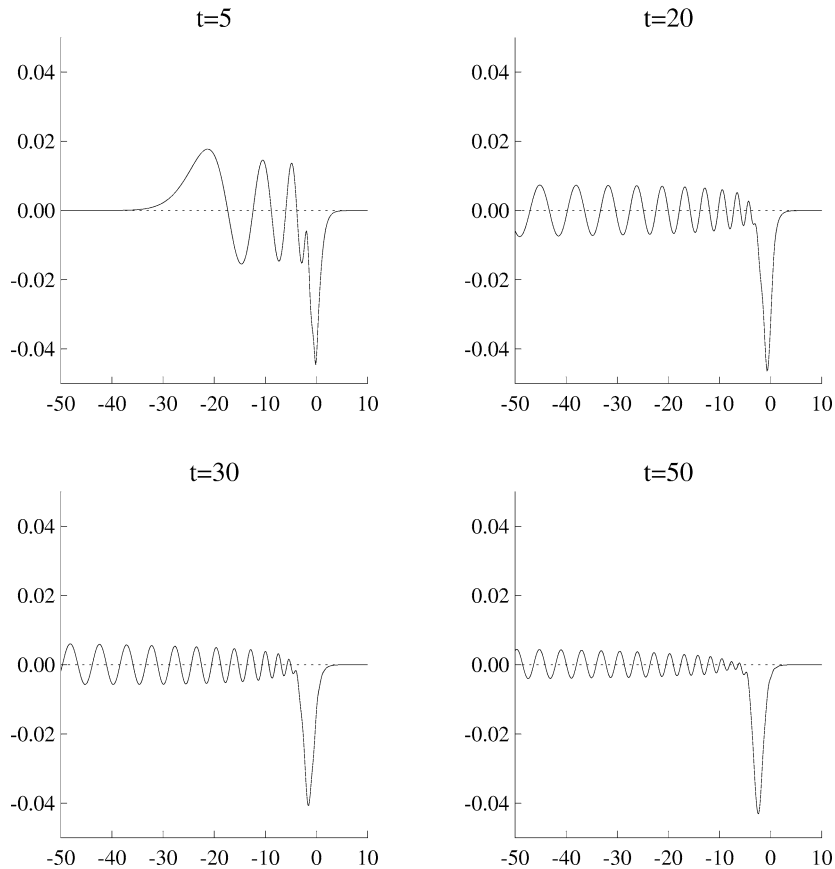

Fig. 5. A close-up of the evolution of the topographic contour, for an anticyclone. The parameter values used are $a = 1,\ L = 1.2$ and $\varepsilon = 0.1$.

$$c_p(k) = -\frac{1}{2\varepsilon(k^2+1)^{1/2}}, \tag{11}$$

$$c_g(k) = -\frac{1}{2\varepsilon(k^2+1)^{3/2}}, \tag{12}$$

where k is the wavenumber in the x-direction. The escarpment acts as a waveguide and both the phase and energy of the waves propagate in the direction of decreasing x, i.e., with shallow water to the right. These dispersive waves are evident for both values of ε. For the weaker vortex, the wavetrain has all the features of a classical dispersive wavetrain (e.g., Whitham [18]): the largest amplitude disturbance is at the head of the wavetrain, and this decays exponentially ahead of the train. The waves behind the head decay algebraically with time leaving a nondispersive disturbance in their wake. This soliton-like disturbance travels with the vortex in its evolution, and consists of fluid which has crossed from the shallow side to the deep side of the escarpment, gaining net cyclonic relative vorticity. In the limit $\varepsilon \to 0$, the nondispersive wave *is* the pseudoimage of the vortex. For the less weak anticyclone in Fig. 6, it is apparent that the nondispersive wave is sufficiently strong to capture the vortex boundary. Fluid is detrained from the vortex and carried along the escarpment. Also note the beginnings of a wake of radiated waves, evidence that the energy of the vortex will be converted to wave energy at longer times. It is apparent that the waves will eventually destroy the vortex, which will cease to exist as a coherent structure at large times. The singular vortex model is unable to capture this feature of the motion.

3.2. Weak cyclones

Fig. 7 compares the evolution of a cyclonic vortex patch near an escarpment with that of an equivalent vortex patch near a wall for $\varepsilon = 0.1,\ \alpha = 1,\ a = 1$ and $L = 1.2$. Again, the pseudoimage description of the vortex evolution is in excellent agreement with the contour dynamics results. Fig. 8 shows a close-up of the evolution of the topographic contour for the same parameter values. Compare this with the motion of an anticyclone with the same parameter value (Fig. 5). The cyclone moves in

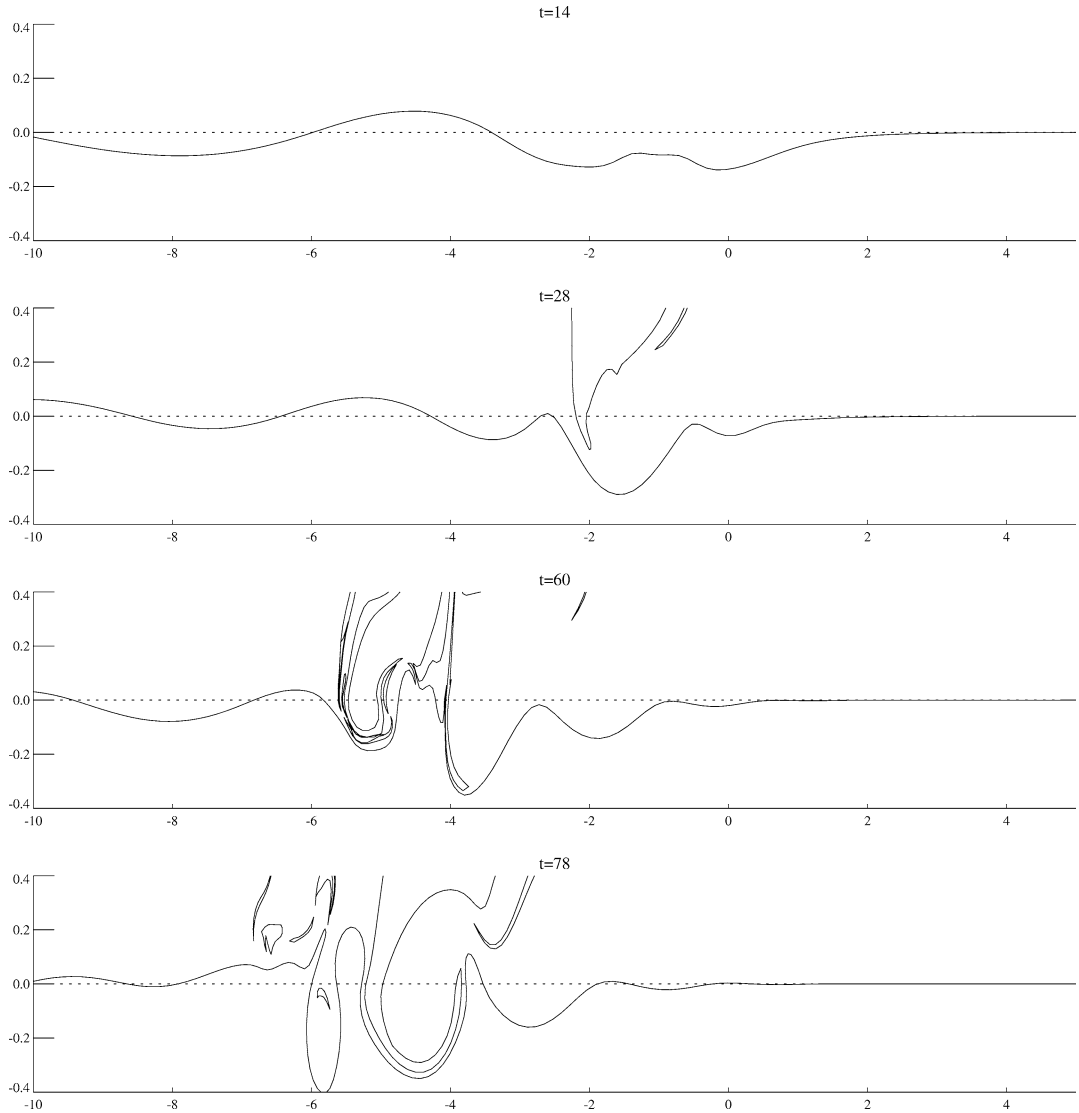

Fig. 6. As Fig. 5, except $\varepsilon = 0.4$.

the direction of increasing x, and the pseudoimage consists of fluid which has crossed from the deep to the shallow side of the escarpment, gaining net anticyclonic relative vorticity. The topographic waves propagate in the opposite direction to the vortex and have no infuence at large times.

For $\varepsilon = 0.2$, (not shown) the pseudoimage description is good for about 20 eddy turnover times, and then deviations from the prediction become pronounced. By $t = 30$ neither the vortex patch boundary, nor its centroid are accurately predicted by the pseudoimage theory. This is in contrast to the anticyclone for the same parameter values, where the linear theory still describes the vortex evolution well. The failure of the pseudoimage theory becomes even more pronounced for $\varepsilon = 0.4$, shown in Fig. 8, where it can be seen that the contour evolution differs significantly from the pseudoimage prediction. The pseudoimage description of the vortex patch evolution is less robust for cyclones than anticyclones. A similar conclusion was reached in the singular vortex case and the mechanism is the same. The initial disturbance "wants" to move west, dispersing as topographic waves. However, in this case the sense of the vortex circulation is such as to counter this tendency and is sufficiently strong to prevent the initial disturbance from moving away from the vicinity of the vortex. In contrast an anticyclone reinforces the westward propagation of the initial disturbance. The primary mechanism for the breakdown of the linear theory for cyclones is the accumulation of anticyclonic relative vorticity near the vortex centre. This is a result of the circulation of the primary vortex driving fluid against the preferred direction of the topographic waves. This anticyclonic relative vorticity is then able,

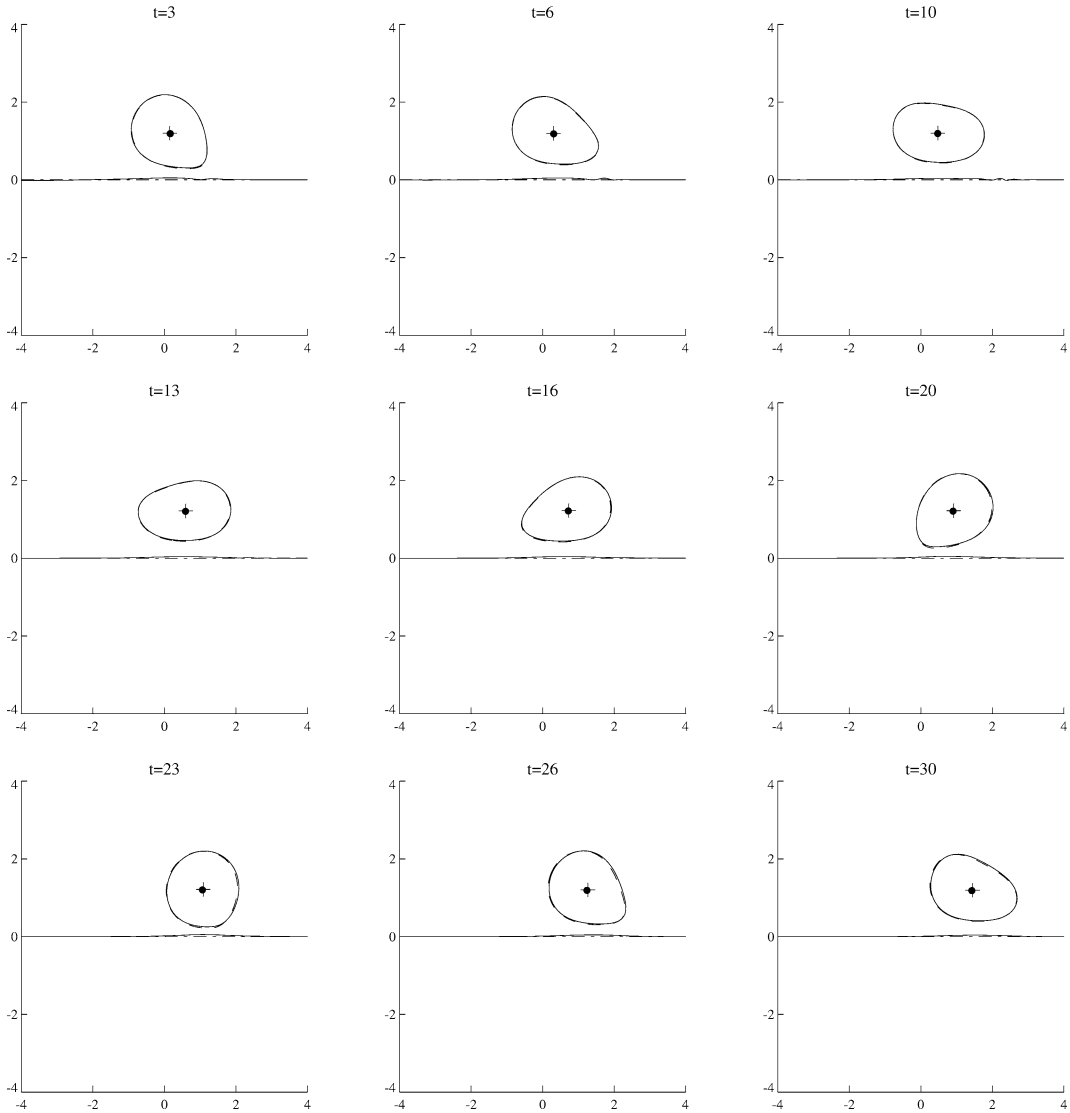

Fig. 7. Comparison of the evolution of a vortex patch near an escarpment (solid line) with that of a vortex patch near a wall (dashed line). The centroid locations are shown by a cross (escarpment) and a dot (wall), and the parameter values used are $\alpha = -1$ (cyclone), $a = 1$, $L = 1.2$ and $\varepsilon = 0.1$.

through a dipole mechanism, to advect the primary vortex northeast. This is clear in Fig. 10 which shows the drift of the vortex centre for cyclones, compared with the analytical prediction in Eq. (10). The discussion of the oscillating nature of the vortex drift for small ε in the previous section applies here; for small ε the pseudoimage describes the motion of weak cyclones for very long times. The vortex drift for larger values of ε is in qualitative agreement with the drift of weak singular cyclone Dunn et al. [5]. Finally note that weak and relatively weak cyclones leave the vicinity of the escarpment, and unlike anticyclones are not decayed by the action of the topographic waves.

4. An intense vortex patch

In Part I it was found that in the limit $S \to 0$, an intense vortex patch remains circular to leading order in S, and that the leading order drift velocity of the vortex centroid is given by

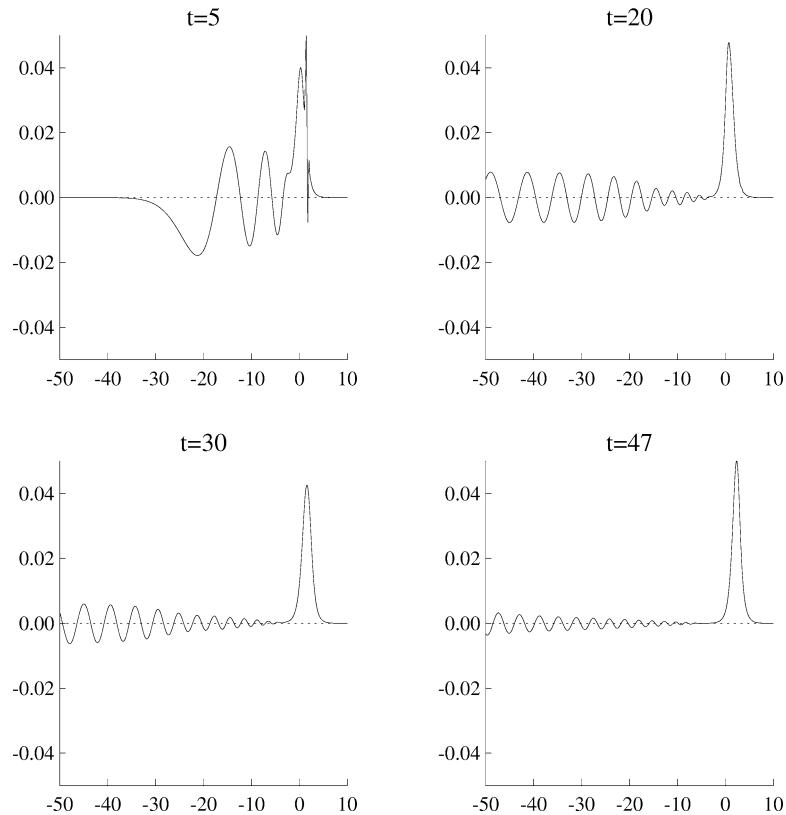

Fig. 8. A close-up of the evolution of the topographic contour, for a cyclone. The parameter values are the same as in Fig. 7.

$$u_1 = \frac{2}{\pi a} I_1(a) \int_{|L|}^{\infty} (\cos bt - 1) K_1(r) \sqrt{r^2 - L^2}\, \mathrm{d}r, \tag{13}$$

$$v_1 = \frac{2}{\pi a} I_1(a) \int_{|L|}^{\infty} \sin bt\, K_1(r) \sqrt{r^2 - L^2}\, \mathrm{d}r, \tag{14}$$

where

$$b(r) = \frac{1}{r}\frac{\partial \psi_0}{\partial r} = \frac{1}{r} \begin{cases} -\alpha a K_1(a) I_1(r), & r \leqslant a, \\ -\alpha a I_1(a) K_1(r), & r > a \end{cases} \tag{15}$$

is the initial angular velocity of the vortex. For $t \gg 1$ but less than $\mathrm{O}(S^{-1})$

$$u_1 \approx -\frac{2 I_1(a)}{a} \exp\bigl(-|L|\bigr) + \mathrm{O}\left(\frac{\log^2 t}{t}\right), \tag{16}$$

$$v_1 \approx \mathrm{O}\left(\frac{\log^2 t}{t}\right). \tag{17}$$

Fig. 11 shows the trajectory of an anticyclone, with $a = 1$, $L = 1.2$ and for $S = 0.05$, 0.1 and 0.2. The displacement of the vortex centroid divided by S is plotted to enable comparison with the analytical prediction. The analytical prediction, shown by the solid line is calculated by fourth order Runge–Kutta and numerical integration of (13), (14). As S is decreased it is evident that the centroid trajectories obtained by contour dynamics approach the theoretical prediction. Note that the contour dynamics trajectories are displaced further to the west than the theory predicts, and this feature is enhanced as S is increased. This is to be expected, since an anticyclone moves southward, i.e., towards the escarpment, and according to Eq. (16) the westward drift increases exponentially as $|L|$ decreases. This feature is not captured by the theory, where $|L|$ is assumed to be constant for $t < \mathrm{O}(S^{-1})$. Fig. 12 shows a similar plot for the trajectory of a cyclone produced by contour dynamics simulations. In this case

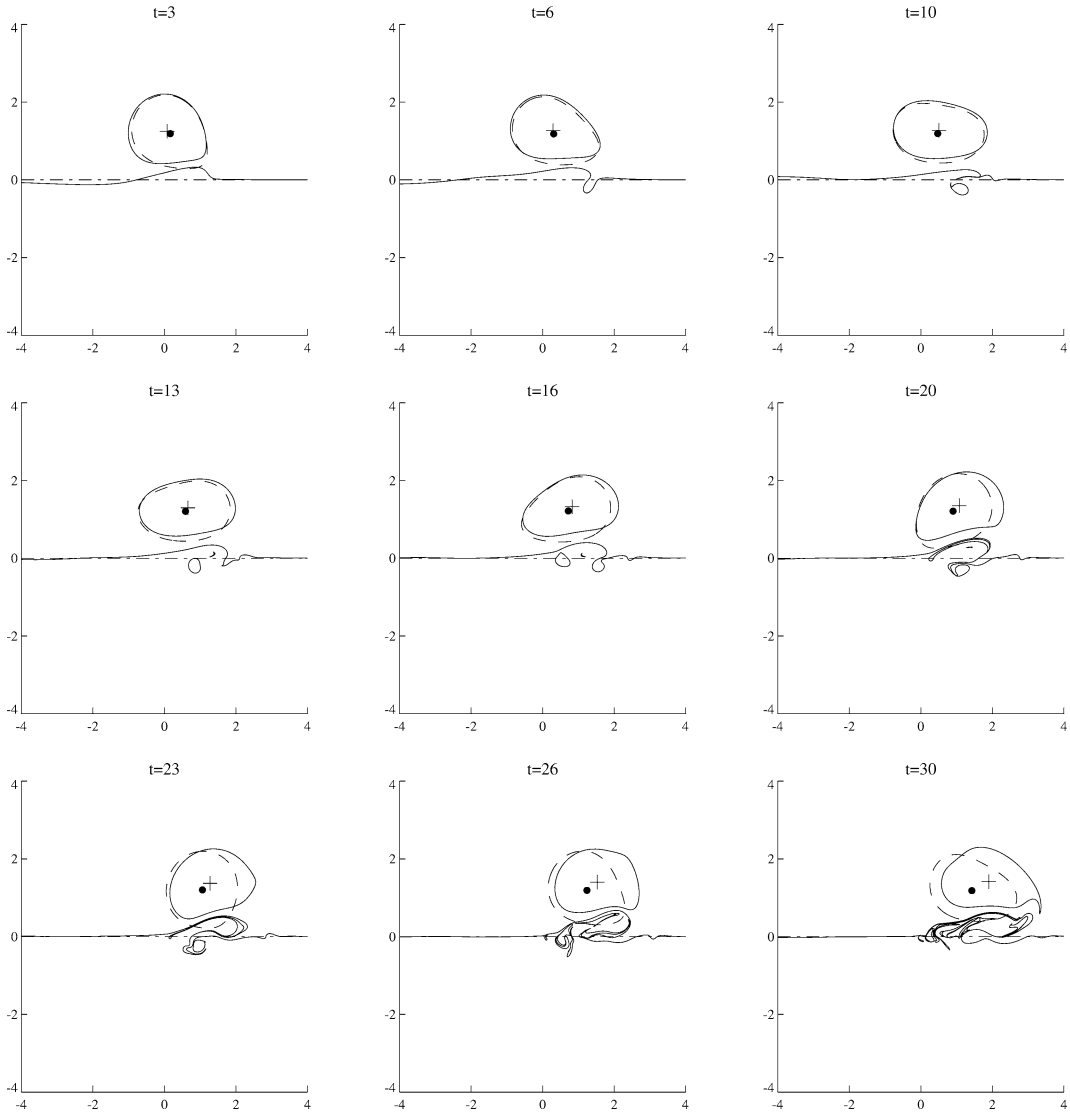

Fig. 9. As Fig. 7, except $\varepsilon = 0.4$.

the numerical calculations produce centroid trajectories which are less displaced in the y-direction than the theory predicts. Again, this is expected since cyclones move away from the escarpment, in turn implying that the magnitude of the x component of the velocity decreases. Finally, note that for both an anticyclone and a cyclone, the trajectory for $S = 0.05$ has a slight 'bump' in comparison with the analytic trajectory. Possible sources of this error are deviations of the vortex shape from circular, and the vortex crossing the escarpment, neither of which were taken into account in the theory. The evolution of the contours for an intense anticyclone is shown in Fig. 13, and the evolution of the contours for an intense cyclone is shown if Fig. 14. In each case $S = 0.1$. The vortex shape remains approximately circular, even up to time $t = 180$. Importantly the vortex remains an isolated, coherent structure, and there is little evidence that wave radiation distorts the vortex even on long time scales.

The topographic contour wraps around the vortex, and consists of weaker potential vorticity than the primary vortex. The resulting differential rotation shields the vortex inside a 'trapped region' (cf. Lam and Dritschel [10], Reznik et al. [15]), inside which the strong axisymmetric swirl velocity of the vortex dominates. The size and shape of the initial vortex is preserved, and the deflected topographic contour serves mainly to steer the intense vortex. Fig. 15 shows the long-term trajectories of a cyclone and an anticyclone with $S = 0.1$ and 0.2, for $0 < t < 180$. First note that the anticyclones experience further zonal drift than the cyclones. This is simply a consequence of them being closer to the topography and thus more susceptible to the

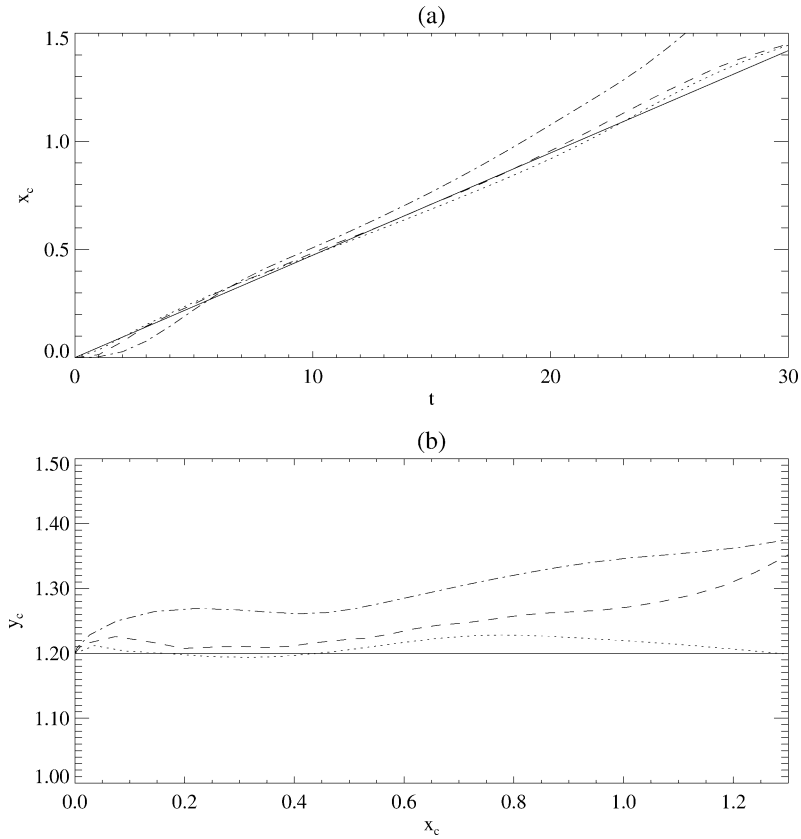

Fig. 10. Comparison of the drift of the weak cyclones with the analytical prediction. The analytical prediction is shown by the solid line. The parameter values used are $a = 1$, $L = 1.2$ and $\varepsilon = 0.1$ (dotted line), $\varepsilon = 0.2$ (dashed line) and $\varepsilon = 0.4$ (dot-dashed line). The x_c-coordinate is shown in (a) as a function of time, and the centroid trajectories in (b).

effects of relative vorticity generation as fluid columns cross the escarpment. Second, both cyclones and anticyclones experience enhanced meridional drift as S increases.

It has been shown that for times up to $t = 30$ the analytic results for the drift of an intense vortex patch near an escarpment predict very well the drift produced by contour dynamics experiments. This agreement improves as $S \to 0$. The large time results produced by contour dynamics simulations reveal two important facts. The first is that the intense vortex patch remains approximately circular for many eddy turnover times. The second is that the meridional drift of the intense vortices increases with S. These two statements hold for both intense cyclones and intense anticyclones.

Why does the vortex remain circular for the large times in the contour dynamics runs presented here? In Part I it was shown that for short times azimuthal mode-1 dominates the flow, and it was shown in the theory that this mode has no leading order effect on the vortex shape. However, it is expected that, at large times, the distortion of the vortex might be significant due to the interaction of higher order normal modes and/or topographic wave radiation. First note that the azimuthal mode-1 (leading order) correction to the relative vorticity is

$$q_1 = q_1^{(s)}(r,t)\sin\theta + q_1^{(c)}(r,t)\cos\theta, \tag{18}$$

where, for $r > |L|$,

$$q_1^{(s)} = \frac{2}{\pi r}\sqrt{r^2 - L^2}(\cos bt - 1), \tag{19}$$

$$q_1^{(c)} = -\frac{2}{\pi r}\sqrt{r^2 - L^2}\sin bt, \tag{20}$$

and for $r < |L|$,

$$q_1^{(c)} = q_1^{(s)} = 0. \tag{21}$$

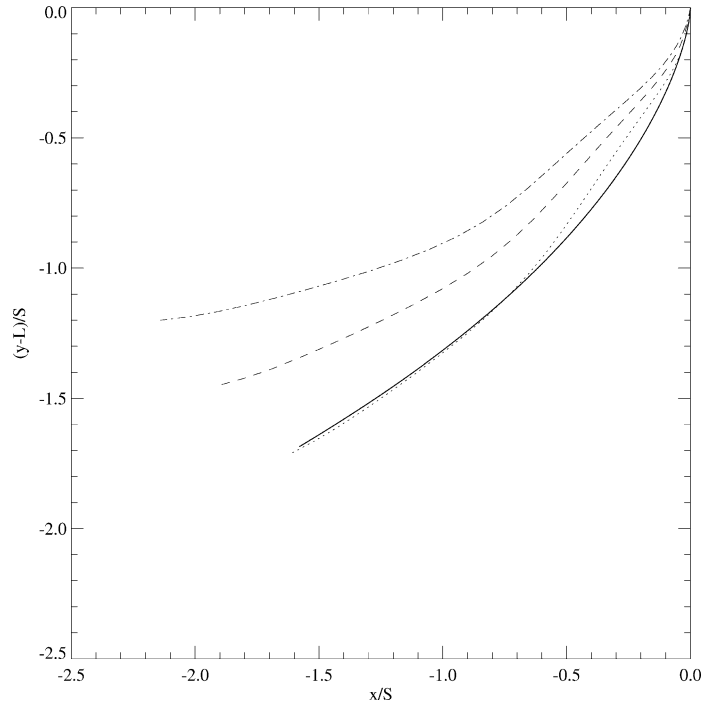

Fig. 11. The trajectory of the vortex centroid for various values of S, for $0 < t < 30$. The parameter values used are $a = 1$, $L = 1.2$ and $\alpha = 1$, i.e., anticyclones. The analytical prediction is shown by the solid line and the contour dynamics results by the dotted line ($S = 0.01$), dashed line ($S = 0.1$) and dot-dashed line ($S = 0.2$).

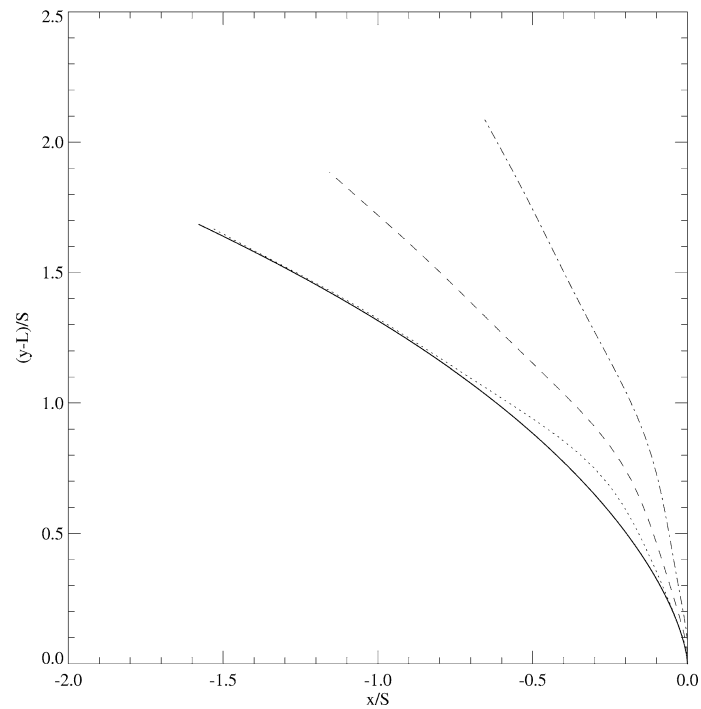

Fig. 12. The trajectory of the vortex centroid for various values of S, for $0 < t < 30$. The parameter values used are $a = 1$, $L = 1.2$ and $\alpha = -1$, i.e., cyclones. The analytical prediction is shown by the solid line and the contour dynamics results by the dotted line ($S = 0.01$), dashed line ($S = 0.1$) and dot-dashed line ($S = 0.2$).

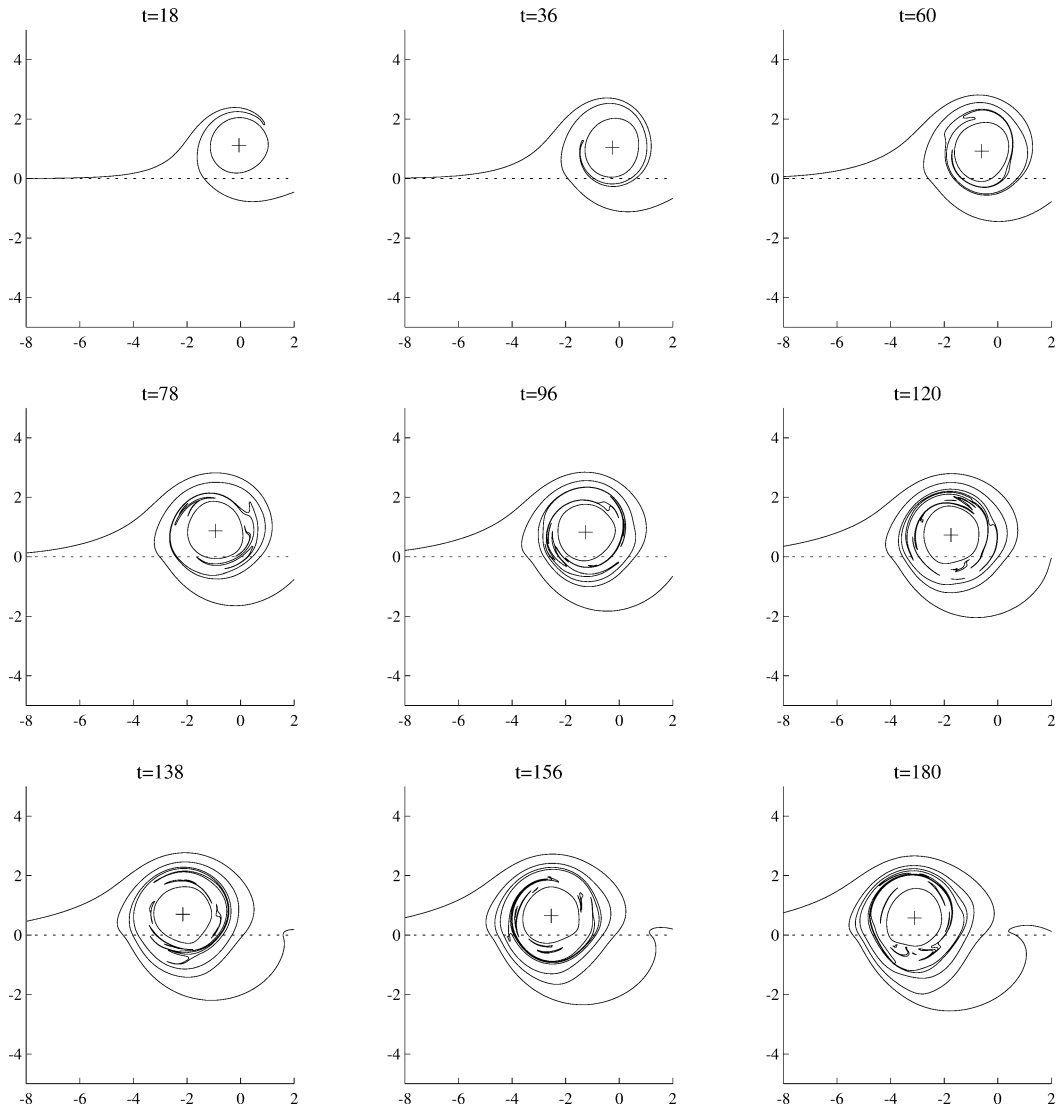

Fig. 13. The contour evolution for an intense anticyclone ($\alpha = 1$). The parameter values used are $a = 1$, $L = 1.2$ and $S = 0.1$.

These equations indicate that, to leading order, none of the redistributed ambient potential vorticity enters the annulus of radius $r < |L|$ around the vortex periphery. This is apparent in Figs. 13 and 14, where the deflected topographic contour wraps around $r = |L|$.

It is evident from Figs. 13 and 14 that the region of axisymmetric flow grows with time. In Part I it was shown that the residual flow practically vanishes in a region $r < r_{\text{div}}$, where r_{div} grows in time. This in turn constrains the growth of the forcing term in the equation for the second order correction to the potential vorticity, q_2. The form of the equation for q_2 implies that the second order streamfunction ϕ_0 consists of an axisymmetric component and a quadrupole component. In the study of Reznik et al. [15], it was found that the axisymmetric part of the second order vorticity correction for an intense vortex patch on the β-plane fills a growing region near the vortex centre, while the quadrupole component decays with time. It is plausible that this is also the case here. The topographic contour is wound around the vortex and consists of potential vorticity which is of different magnitude to the primary vortex. The resulting differential rotation isolates the vortex in a 'trapped region', where the strong axisymmetric rotation keeps the vortex circular. The size of the trapped region grows with time.

Also note, at large times there is a 'trailing eddy' in the wake of the vortex. For the cyclone this eddy consists of fluid which has crossed the escarpment from the deep to the shallow side, and thus consists of anticyclonic relative vorticity.

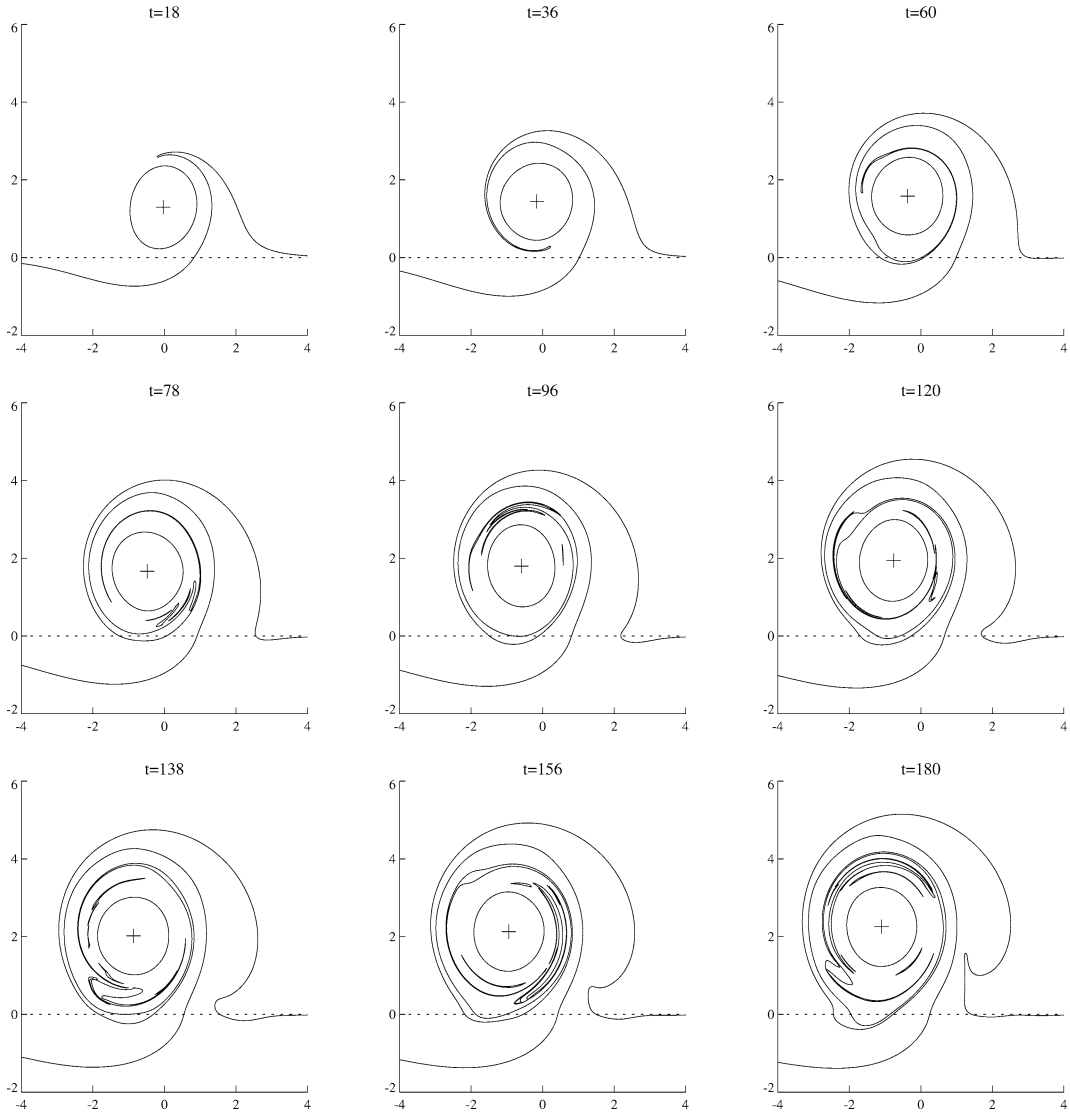

Fig. 14. As Fig. 13, except $\alpha = -1$, i.e., a cyclone.

Similarly, the trailing eddy for the anticyclone consists of fluid with cyclonic relative vorticity. The strength of the trailing eddy increases with S, and enhances meridional motion in the primary vortex. For small values of S the trailing eddy is very weak, and is shielded from the vortex by the trapped zone. As S increases, the strength of the trailing eddy increases, and the size of the trapped zone appears to decrease. For $S = 0.2$ (not shown) there is a marked difference between the evolution of cyclones and anticyclones. In the case of an anticyclone there is still strong wrapping of the topographic contour. The vortex drifts toward the escarpment, and at large times dipole formation is evident. In contrast, the cyclone does not wrap the topographic contour so strongly, and dipole formation is apparent at earlier times. The vortex drifts away from the escarpment, accounting for the weaker interaction of the vortex with the topographic contour. Hence weaker vortices experience greater meridional displacements. Distortion of the vortex shape is also greater for larger S, since the trapped zone is less able to shield the primary vortex from the trailing eddy. Lam and Dritschel [10] show that the β-plane vortices undergoing the greatest meridional drift are moderate intensity ones, and the mechanism is also an eddy in the wake of the vortex.

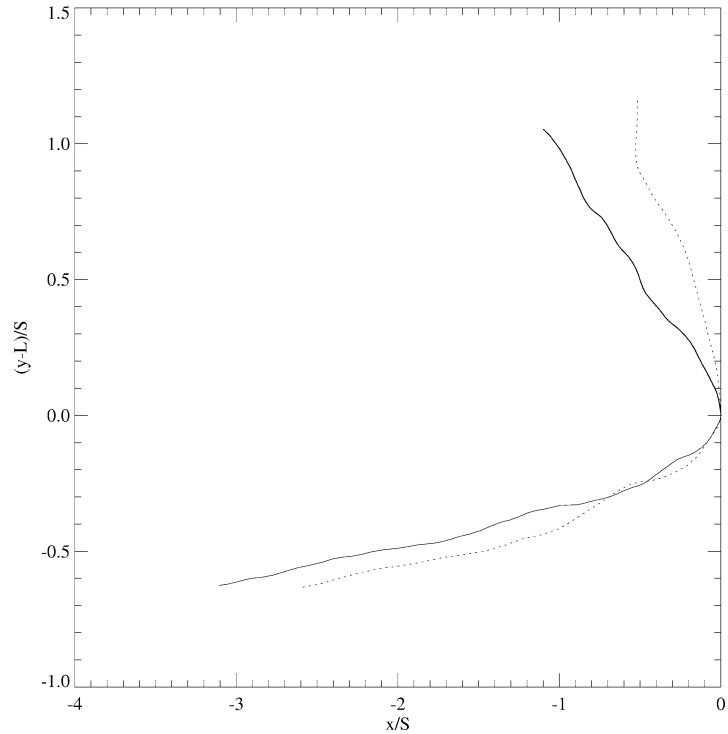

Fig. 15. Contour dynamics trajectories for $0 < t < 180$. The parameter values used are $a = 1,\ L = 1.2$ and $S = 0.2$ (dotted line) and $S = 0.1$ (solid line). The cyclones are northwest moving and the anticyclones are southwest moving.

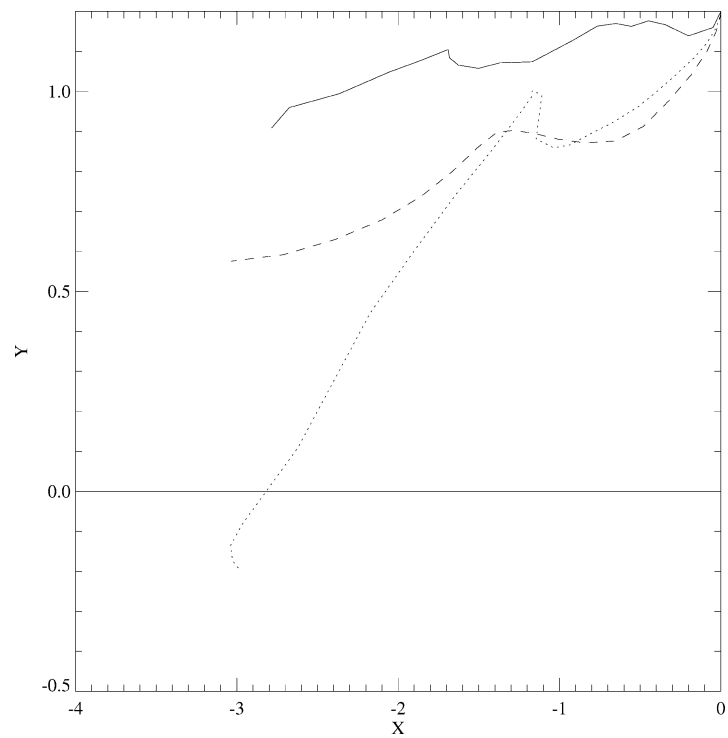

Fig. 16. The trajectories of the moderate anticyclones for $0 < t < 60$. The parameter values used are $a = 1,\ L = 1.2$ and $S = 2$ (solid line), $S = 1$ (dotted line) and $S = 0.5$ (dashed line).

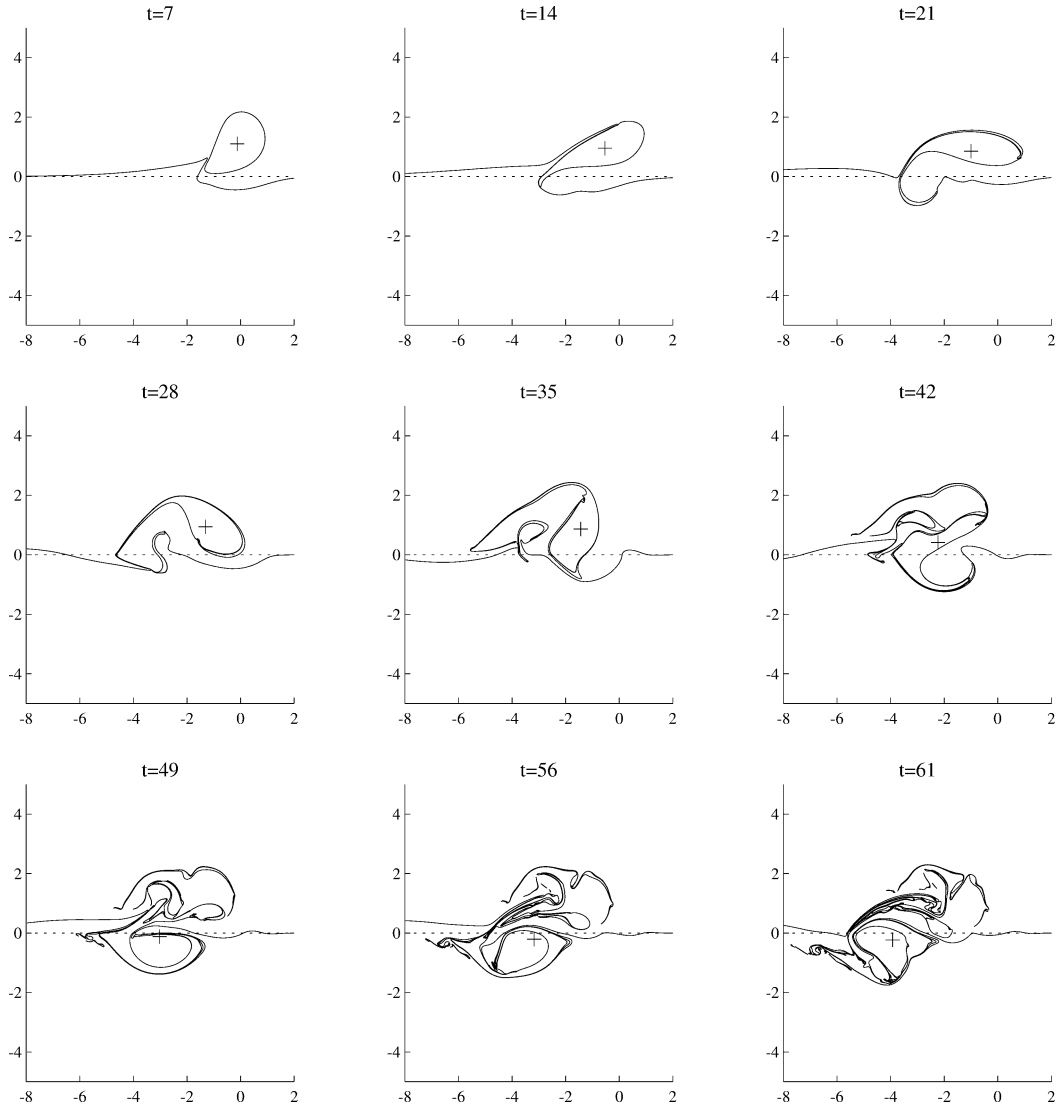

Fig. 17. The contour evolution for a moderate anticyclone ($\alpha = 1$). The parameter values used are $a = 1$, $L = 1.2$ and $S = 1$.

5. A moderate intensity vortex patch

In this section contour dynamics results for a moderate intensity vortex patch ($S \approx 1$) are presented. Three particular parameter values are chosen: $S = 2$ (a moderately weak vortex), $S = 1$ (a moderate vortex) and $S = 0.5$ (a moderately intense vortex). The predominant behaviour is dipole formation: the primary vortex forms one cell, and the other cell consists of fluid which has crossed the escarpment and gained potential vorticity as a result. The trajectories are the looping paths characteristic of dipoles with cells of differing circulations. The simulations demonstrate similar behaviour to recent numerical and experimental work.

5.1. Moderate anticyclones

Fig. 16 shows the trajectories of the centroid for a moderate anticyclone of various strengths, for $0 < t < 60$. The x-component of the vortex drift is approximately the same for each value of S. The moderately weak ($S = 2$) anticyclone drifts predominantly in the x-direction, but the escarpment-ward drift is greater than that seen for weak anticyclones. The moderate ($S = 1$) anticyclone undergoes the greatest meridional drift, crosses the escarpment and begins to turn east at later times. The moderately strong ($S = 0.5$) anticyclone follows a generally southwestward trajectory, similar to an intense anticyclone.

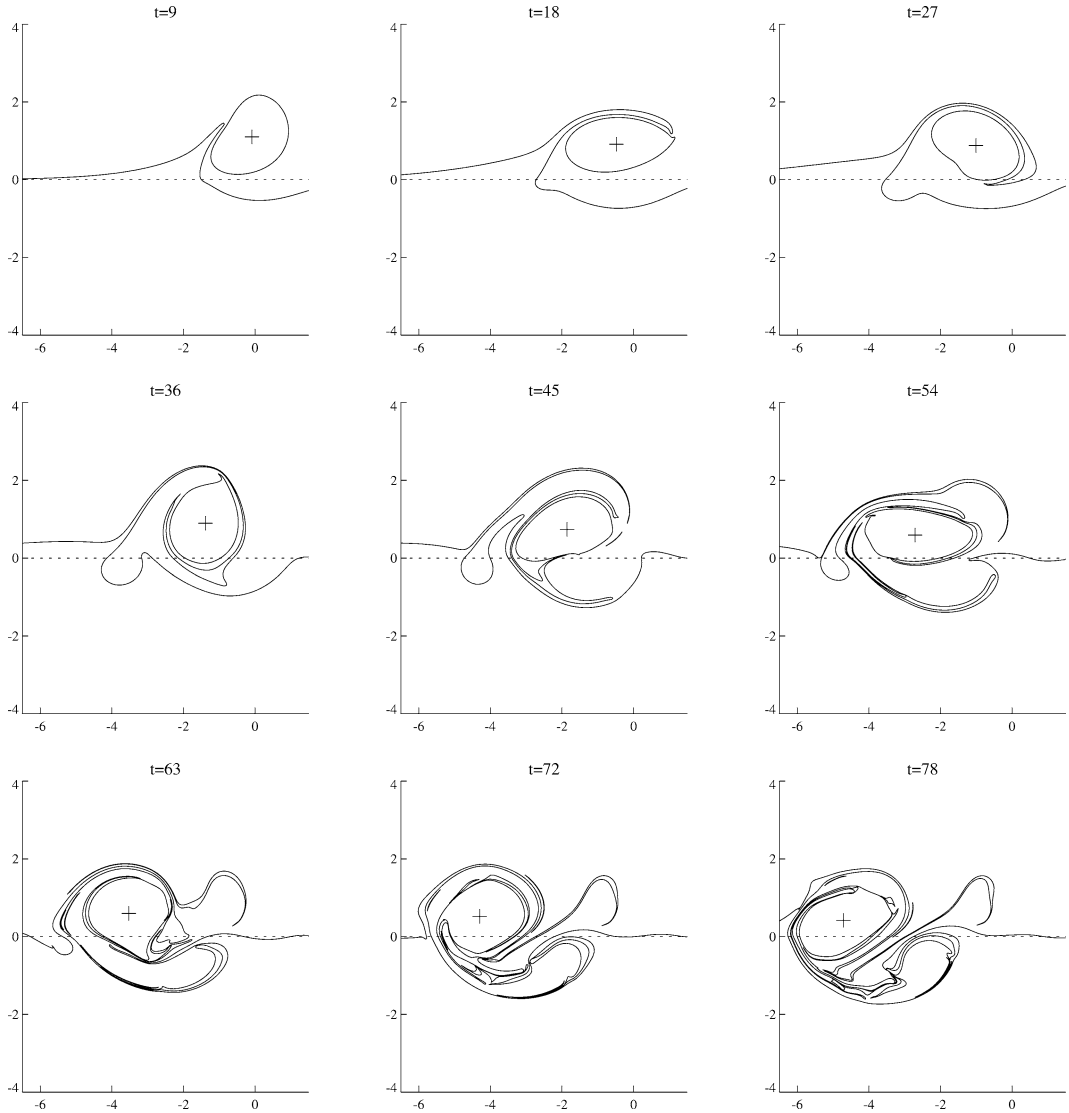

Fig. 18. The contour evolution for a moderately intense anticyclone ($\alpha = 1$). The parameter values used are $a = 1$, $L = 1.2$ and $S = 0.5$.

Fig. 17 shows the contour evolution for the case $S = 1$. From the outset of the motion, fluid is detrained from the vortex by the deforming topographic contour. The vortex is rapidly distorted and the trailing cyclonic relative vorticity induces significant escarpment-ward drift of the vortex. By $t = 54$ the vortex has ceased to exist as a coherent structure, and has merged with the topographic contour. The evolution of the moderately weak anticyclone (not shown) is similar, and the vortex is ripped apart at large times. The moderately intense anticyclone (Fig. 18) is less this distortion. The trailing cyclonic eddy causes escarpment-ward drift of the vortex, but the vortex remains a relatively coherent structure. At later times a dipole has formed, and this dipole continues the general southwest migration.

Zavala Sanson et al. [19] have investigated the motion of barotropic vortices near an escarpment, both experimentally and numerically, and have found that an anticyclone which moves towards 'step-down' topography crosses the escarpment. Dunn et al. [5] found similar behaviour for a moderate intensity singular vortex, and identified the mechanism for the behaviour as the formation of dipole like structures. The results given here for a moderate intensity vortex patch are consistent with these studies, and it appears that the dipole formation is responsible for the observed vortex trajectories. It should be noted that the singular vortex can not be ripped apart as a result of its interaction with the topographic contour. Moreover Dunn [4] showed that even for small patches, the singular vortex model only predicts the trajectory for one or two eddy turnover times.

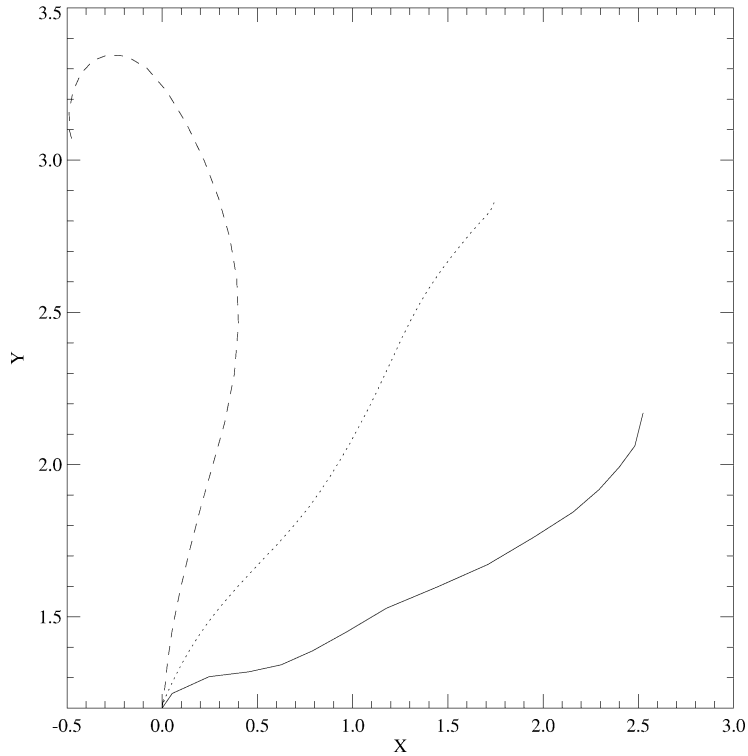

Fig. 19. The trajectories of the moderate cyclones for $0 < t < 60$. The parameter values used are $a = 1$, $L = 1.2$ and $S = 2$ (solid line), $S = 1$ (dotted line) and $S = 0.5$ (dashed line).

5.2. Cyclones

Fig. 19 shows the trajectories of the centroid for the moderate cyclones. In all cases the vortex drifts in the opposite direction to the topographic waves and away from the escarpment. The trajectory of the moderately intense cyclone ($S = 0.5$) shows the beginnings of a looping motion. Dunn et al. [5] found that moderate singular cyclones follow looping trajectories away from the escarpment, the looping being characteristic of a dipole structure whose constituent cells differ in magnitude.

The dipole formation is evident in Figs. 20 and 21, which show the contour evolution for $S = 1$ and 0.5, respectively. A dipole is formed as the primary cyclonic vortex becomes associated with the patches of anticyclonic relative vorticity, produced due to fluid columns crossing the escarpment from the deep to the shallow side. Zavala Sanson et al. [19] found that barotropic cyclones approaching a step-down escarpment are 'back-reflected', precisely the same behaviour observed here.

6. Discussion and conclusions

Contour dynamics has been used to study the motion of a vortex patch near an escarpment for the full range of values of the vortex intensity, S. The algorithm integrates the full nonlinear equation of motion. The asymptotic results obtained in Part I for the motion of weak and intense vortices have been checked, and the intermediate case of a moderate intensity vortex has been studied.

The evolution of a weak vortex patch is well described by the pseudoimage for many eddy turnover times, and its motion is well predicted by that of an equivalent vortex near a wall. Wave radiation for anticyclones (which drift in the same direction as the topographic waves) appears insignificant for small ε. This might be expected, given the weak singular vortex results of Dunn et al. [5], who have shown that wave induced drift is $O(e^{-1/\varepsilon})$, a result of the vortex travelling at the topographic *short* wave velocity. Since the short waves are the least energetic it is reasonable to assume that the effects of wave radiation are not evident for the times of the runs given. For larger values of ε it has been shown that wave radiation is significant and causes enhanced drift perpendicular to the escarpment. It is worth highlighting that the singular weak anticyclone is *unable* to change its shape, and for values of ε comparable to those discussed here, the weak, singular anticyclone responds to wave radiation

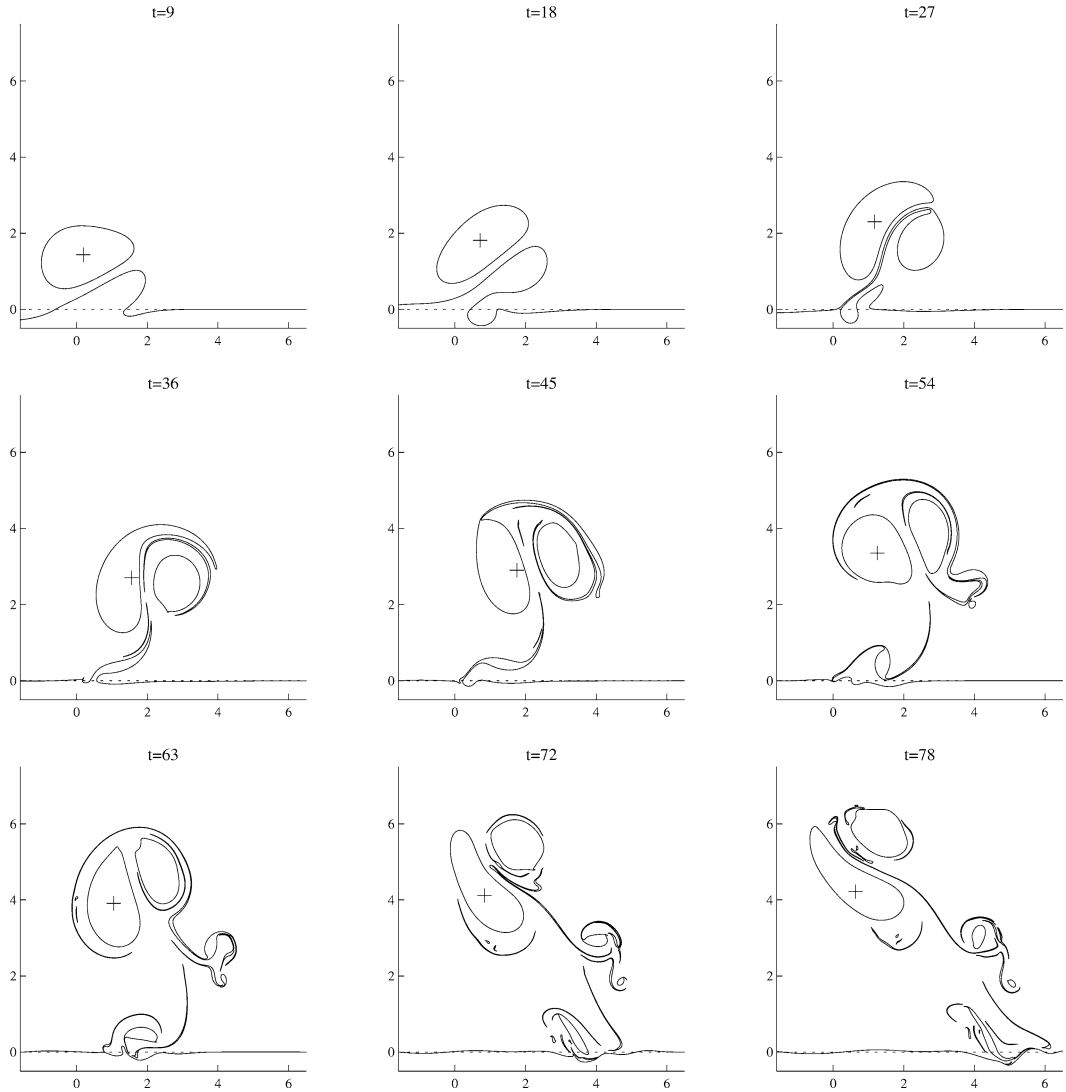

Fig. 20. The contour evolution for a moderate intensity cyclone ($\alpha = 1$). The parameter values used are $a = 1$, $L = 1.2$ and $S = 1$.

through meridional drift only. The anticyclonic vortex patch, on the other hand, decays via stripping. This stripping is due in part to wave radiation, but this type of vortex filamentation is associated with the local shear in the flow.

The weak vortex theory is less robust for cyclonic vortex patches, and breaks down for $\varepsilon \approx 0.2$. Nonlinear effects are far more significant for cyclones than anticyclones, and this is due to the circulation of the vortex competing with the preferential direction of propagation of the topographic waves. The circulation of the vortex patch induces a secondary anticyclonic circulation in its vicinity, and the dipolar nature of this structure causes a northeastward drift of the primary vortex.

There is no β-plane analogy for the evolution of a weak vortex patch near an escarpment; the pseudoimage description is an artifact of the discontinuous topographic gradient, and weak vortices near an escarpment are long lived, by comparison with weak vortices on the β-plane, which drift west, regardless of the sense of the circulation, and which decay rapidly as the result of Rossby wave radiation. The figures of Lam and Dritschel [10] illustrate this process well.

The theory of Part I also accurately predicts the motion of an intense vortex patch as S decreases. It was suggested by the theory that the singular vortex model would predict the trajectory of the vortex centre, a result arising from the fact that the vortex remains circular to leading order. Contour dynamics results confirmed this to be the case, and it was found that cyclones (respectively anticyclones) drift northwest (southwest) as a result of the formation of a secondary dipole. The westward drift speed is within the range of possible phase speeds of the topographic waves. However, for small values of S wave radiation appeared to have a negligible effect on either the vortex shape or the meridional velocity.

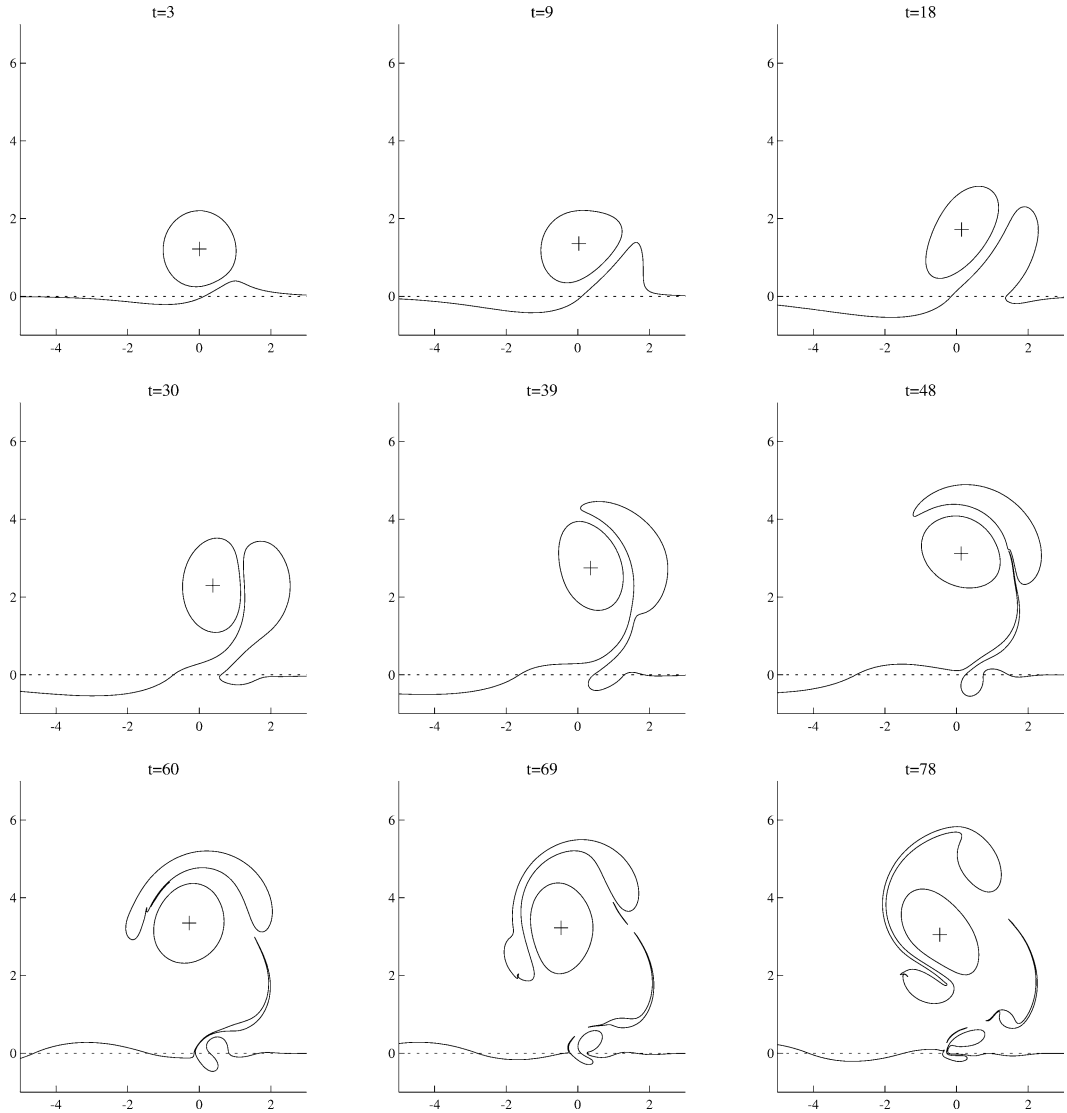

Fig. 21. As for Fig. 20, except $S = 0.5$, i.e., a moderately intense cyclone.

The curved westward paths of the intense vortices is very similar to those of intense β-plane vortices (e.g., Firing and Behaviour [7], Sutyrin and Flierl [17]). The mechanism for the motion is similar to the β-gyres, i.e., the establishment of dipolar secondary circulations generated by the vortex pushing fluid columns across the potential vorticity gradient. Lam and Dritschel [10] have applied the Contour-Advective semi-Lagrangian (CASL) algorithm of Dritschel and Ambaum [3], to the motion of initially circular vortices on the β-plane, obtaining high-resolution, long-time runs. A trapped region around intense vortices was identified, as well as a trailing eddy. The trapped region has also been elucidated in the analytical work of Reznik et al. [15]. Both of these features have been observed in the present work an the may be characteristic of interactions of intense vortices with potential vorticity gradients.

Weak and intense vortices near an escarpment maintain their existence as isolated, coherent structures. Shape deformation is important for moderate intensity vortices. This feature is, of course, not captured by the singular vortex model of Dunn et al. [5]. Moderate anticyclones eventually have their fluid detrained by the topographic waves and cease to exist as coherent structures at large times. A moderately strong anticyclone moves southwest, as a result of dipole formation and at large times crosses to the deep side of the escarpment.

In contrast, the moderate cyclones exhibit similar qualitative features to the moderate singular cyclones. The primary vortex remains a coherent structure, and is steered away from the escarpment as a result of dipole formation. The dipole formation

seems more robust for cyclones and is a result of the motion away from the escarpment, and hence away from the influence of the topography.

The moderate vortex patch undergoes greater meridional drift than either the weak or intense vortices. A similar conclusion for moderate intensity β-plane vortices was reached by Lam and Dritschel [10]. There is however an important exception. The moderate vortex near an escarpment does not have an associated trapped zone, except for, arguably, the moderately strong cyclone. This is due to the vortex being a finite distance from the topography, and thus being unable to wrap up the contour efficiently. Instead the trailing eddy dominates the motion and causes the enhanced meridional motion.

The results for the moderate vortex are in agreement with those of Zavala Sanson et al. [19], who showed in laboratory and numerical experiments, that an anticyclone approaching an escarpment from the shallow side proceeded to cross the escarpment, and a cyclone approaching an escarpment from the shallow side is back-reflected as a result of dipole formation. One may speculate that dipole formation as a result of vortex interaction with potential vorticity gradients is a generic feature of geophysical fluid dynamics.

Acknowledgements

This work was supported by NERC under grant GT4/95/206/M. I am grateful to Roger Grimshaw and David Dritschel who provided preprints of Reznik et al. [15] and Lam and Dritschel [10] in 1998, before they appeared in the open literature. Without these papers I would not have undertaken this study as part of my thesis. I am also grateful to Robb McDonald and Ted Johnson for discussions of these results. Finally I would like to thank the referees whose comments have greatly improved this two part paper.

References

[1] G.I. Bell, Interaction between vortices and waves in a simple model of geophysical flow, Phys. Fluids A 2 (1989) 575–586.
[2] D.G. Dritschel, Contour surgery: a topological reconnection scheme for extended integrations using contour dynamics, J. Comput. Phys. 77 (1988) 240–266.
[3] D.G. Dritschel, M.H.P. Ambaum, A contour-advective semi-Lagrangian numerical algorithm for simulating fine-scale conservative dynamical fields, Quart J.R. Met. Soc. 123 (1997) 1097–1130.
[4] D.C. Dunn, Vortex interactions with topographic features in geophysical fluid dynamics, Ph.D. thesis, University College London, 2000.
[5] D.C. Dunn, N.R. McDonald, E.R. Johnson, The motion of a singular vortex near an escarpment, J. Fluid Mech. 448 (2001) 335–365.
[6] D.C. Dunn, N.R. McDonald, E.R. Johnson, The evolution of an initially circular vortex near an escarpment. Part I: analytical results, Eur. J. Mech. B Fluids (2002) 657–675.
[7] E. Firing, R. Beardsley, The behaviour of a barotropic eddy on a β-plane, J. Phys. Ocean. 6 (1976) 57–65.
[8] E.R. Johnson, Starting flow for an obstacle moving transversely in a rapidly rotating fluid, J. Fluid Mech. 149 (1984) 71–88.
[9] E.R. Johnson, M.K. Davey, Free-surface adjustment and topographic waves in coastal currents, J. Fluid Mech. 219 (1990) 273–289.
[10] J.S.-L. Lam, D.G. Dritschel, On the beta-drift of an initially circular vortex patch, J. Fluid Mech. 436 (2001) 107–129.
[11] N.R. McDonald, Motion of an intense vortex near topography, J. Fluid Mech. 367 (1998) 359–377.
[12] N.R. McDonald, D.C. Dunn, Some interactions of a vortex with a seamount, Nuovo Cimento C 22 (1999) 885.
[13] R.T. Pierrehumbert, A family of steady, translating vortex pairs with distributed vorticity, J. Fluid Mech. 99 (1980) 129–144.
[14] G.M. Reznik, Dynamics of singular vortices on a beta-plane, J. Fluid Mech. 240 (1992) 405–432.
[15] G.M. Reznik, R. Grimshaw, E.S. Benilov, On the long term evolution of an intense localised divergent vortex on the β-plane, J. Fluid Mech. 422 (1998) 249–280.
[16] M.E. Stern, G.R. Flierl, On the interaction of a vortex with a shear flow, J. Geophys. Res. 92 (1987) 10733–10744.
[17] G.G. Sutyrin, G.R. Flierl, Intense vortex motion on the beta plane: development of the beta gyres, J. Atmos. Sci. 51 (1994) 773–790.
[18] G.B. Whitham, Linear and Nonlinear Waves, Wiley, 1974.
[19] I. Zavala Sanson, G.J.F. van Heijst, J.J.J. Doorschoot, Reflection of barotropic vortices from a step-like topography, Nuovo Cimento C 22 (2000) 909–930.